DMD Fast Forward. Published on February 11, 2016 as DOI: 10.1124/dmd.115.068874
This article has not been copyedited and formatted. The final version may differ from this version.



**Title Page**

# Integrin Receptors Play a Key Role in the Regulation of Hepatic Cytochrome P450 3A

**Kristina Jonsson-Schmunk, Piynauch Wonganan, Jin Huk Choi, Shellie M. Callahan and Maria A. Croyle**

Division of Pharmaceutics, College of Pharmacy (K. J.-S., P.W., J.-H. C., S. M. C. and M. A. C.) and Center for Infectious Disease (M. A. C.), The University of Texas at Austin, Austin, TX, 78712, U.S.A.

**Running Title Page**

**Running title:** Integrins and Drug Metabolism

**Address correspondence to:**
Maria A. Croyle, R.Ph., Ph.D.
The University of Texas at Austin
College of Pharmacy, PHR 4.214D
2409 W. University Ave.
Austin, TX 78712-1074
Tel: 512-471-1972
Fax: 512-471-7474
E-mail: macroyle@austin.utexas.edu

Text pages: 42

Tables: 1

Figures: 8

References: 65

Abstract words: 247 words

Introduction words: 744 words

Discussion words: 1451 words

**Abbreviations:** CYP, cytochrome P450; PXR, pregnane X receptor; CAR, constitutive androstane receptor; RXRα, retinoid X receptor alpha; NADPH, nicotinamide adenine dinucleotide phosphate reduced form, HPLC, high-pressure liquid chromatography; MOI, multiplicity of infection; LPS, lipopolysaccharide; RGD, arginine-glycine-aspartic acid; RGE, arginine-glycine-glutamic acid; NFκB, nuclear factor kappa B; PI3K, phosphoinositide 3-kinase; Jak-Stat, Janus kinase/signal transducers and activators of transcription; PKC protein kinase C; ECM, extracellular matrix; AdCAR, coxsackie- and adenovirus receptor; HSPGs, heparan sulfate proteoglycans; TLRs, Toll-like receptors.

**Abstract**

Landmark studies describing the effect of microbial infection on the expression and activity of hepatic cytochrome P450 3A (CYP3A) used bacterial lipopolysaccharide (LPS) as a model antigen. Our efforts to determine if these findings were translatable to viral infections led us to observations suggesting that engagement of integrin receptors is key in the initiation of processes responsible for changes in hepatic CYP3A4 during infection and inflammation. Studies outlined in this manuscript were designed to evaluate if engagement of integrins, receptors commonly utilized by a variety of microbes to enter cellular targets, is vital in the regulation of CYP3A in the presence and the absence of virus infection. Mice infected with a recombinant adenovirus (AdlacZ) experienced a 70% reduction in hepatic CYP3A catalytic activity. Infection with a mutant virus with integrin-binding RGD sequences deleted from the penton base protein of the virus capsid (AdΔRGD) did not alter CYP3A activity. CYP3A mRNA and protein levels in AdlacZ-treated animals were also suppressed while those of mice given AdΔRGD were not significantly different from uninfected control mice. Silencing of the integrin β-subunit reverted adenovirus-mediated CYP3A4 suppression *in vitro.* Silencing of the α-subunit did not. Suppression of integrin subunits had a profound effect on nuclear receptors PXR and CAR while RXRα was largely unaffected. This is the first time extracellular receptors, like integrins, have been indicated in the regulation of CYP3A. This finding has several implications due to the important role of integrins in normal physiological process and in many disease states.

DMD Fast Forward. Published on February 11, 2016 as DOI: 10.1124/dmd.115.068874
This article has not been copyedited and formatted. The final version may differ from this version.



## Introduction

The CYP3A enzyme family is unique in its capability of metabolizing a variety of compounds that span 38 different therapeutic indications in addition to natural biomolecules (steroids, cholesterol), toxins and carcinogens (Sevior, 2012). The performance of this rather diverse group of enzymes is also highly sensitive to microbial infection (Croyle, 2009; Gandhi, 2012). While the primary paradigm of the field attributed this effect to the production of interferons, cytokines and chemokines (Zanger, 2013), we found that the expression and function of hepatic CYP3A2 in the rat is suppressed for 14 days after a single dose of a recombinant adenovirus, long after these inflammatory mediators dissipate (Callahan, 2005). Additional studies revealed that reducing the immunogenicity of the virus by chemical and physical means did not mitigate this effect (Callahan, 2008a). These findings, coupled with a clinical report detailing dramatic changes in hepatic CYP3A in response to cytokines produced during active infection while minimal changes were found in patients given exogenous cytokines in the absence of infection (Reiss, 1998), suggest that the presence of the microbial pathogen itself plays a role in the process that alters CYP3A during infection.

In an effort to identify the underlying mechanism by which virus infection alters CYP3A expression and function, gene expression patterns in the liver of animals given a single dose of different live and inactivated recombinant adenoviruses were analyzed over time using signal transduction microarrays (Figure 1, Table 1). Global evaluation of data identified 5 pathways that were consistently upregulated for 14 days after infection. The nuclear factor kappa B (NFκB) pathway was the most profoundly affected by all viruses when compared to saline-treated controls. Other pathways upregulated by the presence of virus (in descending order of

intensity) were: the phosphoinositide 3-kinase (PI3K), Janus kinase/signal transducers and activators of transcription (Jak-Stat), protein kinase C (PKC) and retinoic acid pathways. Each of these pathways has been documented to alter the expression and function of hepatic CYP3A in some capacity (Ding, 2005; Wang, 2008; Zangar, 2008; Pondugula, 2009; Kacevska, 2013). Further evaluation of this data with that from a pilot study in which CYP3A activity was suppressed in primary hepatocytes treated with an arginine-glycine-aspartic acid (RGD) peptide known to engage integrins in the absence of virus infection (Callahan, 2008a), solidified our hypothesis that engagement of integrin receptors by the virus at the start of infection may be sufficient to initiate processes that suppress hepatic CYP3A.

The integrin family consists of 24 membrane-spanning receptors. Each receptor consists of a heterodimeric, non-covalently associated combination of one of the 18 alpha and one of the 8 beta protein subunits (Campbell, 2011). In humans, integrins are expressed in almost every cell type and primarily mediate adhesion to the extracellular matrix (ECM) but also play a role in embryonic development and cell differentiation (Desgrosellier, 2010). All integrin subunits have a single membrane-spanning helix and usually a short unconstructed cytoplasmic tail (Shattil, 2010). Integrins are also employed by a variety of enveloped and non-enveloped viruses (Stewart, 2007), fungi (Forsyth, 1998) and bacteria (Hauck, 2012) to gain entry and establish infection in host cells. Adenoviruses bind to several extracellular receptors, including integrins. Well-characterized integrins responsible for cellular entry of human adenovirus are integrin receptors $\alpha_v\beta_3$ and $\alpha_v\beta_5$. Both integrin subtypes promote virus internalization through interaction with a conserved RGD motif in the adenovirus penton base (Wolfrum, 2013). Integrin receptors are attractive targets for pathogens in that they play a key role in endocytosis and intracellular

trafficking throughout the cytoplasm (Caswell, 2009). Integrins are also involved in numerous disease states including cancer, thrombosis, multiple sclerosis, psoriasis, asthma, ulcerative colitis and acute coronary syndromes (Cox, 2010). Hence, integrin receptors have evolved during the last few years as exciting therapeutic targets with approximately 300 anti-integrin drugs in various stages of clinical testing (Goodman, 2012).

Given the importance of integrins in infection and other non-infectious disease states, the primary goal of the studies summarized in this manuscript was to further solidify the hypothesis that integrin receptors influence the expression and function of hepatic cytochrome P450 3A *in vivo*. This was achieved by infecting mice with two recombinant adenoviruses that differ only in their ability to bind integrin receptors (Shayakhmetov, 2005a). A secondary goal of these studies was to identify specific integrin receptor subunits responsible for changes in CYP3A. *In vitro* assessment of CYP3A activity and expression after knockdown of various α- and β- subunits of integrin receptors in a novel human-derived hepatocyte cell line (Wonganan, 2014) allowed us to prioritize the role each plays in the regulation of CYP3A and several transcription factors known to moderate this enzyme. To our knowledge, this is the first report describing a role for these ubiquitous receptors in the regulation of drug metabolism *in vivo* and in human hepatocytes.

## Materials and Methods

**Reagents.** Acetopromazine was purchased from Fort Dodge Laboratories (Atlanta, GA). Ketamine was purchased from Pfizer (New York, NY). Phosphate-buffered saline (PBS), ethylenediaminetetraacetic acid (EDTA), glucose-6-phosphate, glucose-6-phosphate dehydrogenase, β-nicotinamide adenine dinucleotide phosphate sodium salt hydrate (NADP), 11α-hydroxyprogesterone and testosterone were purchased from Sigma-Aldrich (St. Louis, MO). Protogel® acrylamide was purchased from National Diagnostics (Atlanta, GA). Testosterone metabolite standards were purchased from Steraloids Inc. (Wilton, NH). Oligonucleotide primers were custom synthesized by Sigma Life Science (Woodlands, TX). All other chemicals were of analytical reagent grade and purchased from EMD Chemicals (Gibbstown, NJ) unless specified otherwise.

**Recombinant Adenovirus Production.** All viruses were amplified in human embryonic kidney (HEK) 293 cells except for the helper-dependent adenovirus (HDAd) which was amplified in 293Cre cells with the use of the helper virus, AdLC8cLuc, and purified from secondary lysates as previously described (Croyle, 2005). Viruses were purified by banding twice on cesium chloride gradients and desalted on Econo-Pac 10 DG disposable chromatography columns (BioRad, Hercules, CA) equilibrated with sterile 100 mM phosphate buffered saline (pH 7.4). Positive fractions were collected and the number of virus particles determined using the method of Maizel et al. (Maizel, 1968) with the following formula: virus particles/ml = (absorbance at 260 nm) × (dilution factor) × $1.1 \times 10^{12}$.

**Modification of Recombinant Adenoviruses.** Virus capsid proteins were covalently modified with monomethoxypoly(ethylene) glycol, activated by tresyl chloride (Sigma Aldrich, St. Louis, MO) according to an established protocol (Croyle, 2000). Approximately 15,445 PEG molecules were associated with each virus particle in the studies outlined here as determined by a PEG-biotin assay (Croyle, 2005). Inactive control virus was produced by mixing freshly purified virus with riboflavin (50 μM, final concentration) and subsequent exposure of the mixture to UV light for one hour according to a protocol established in our laboratory (Callahan, 2008b). Virus inactivation was confirmed by limiting dilution and infection of HeLa cells.

**Administration of Adenoviral Vectors.** All procedures were approved by the Institutional Animal Care and Use Committee of The University of Texas at Austin and are in accordance with the guidelines established by the National Institutes of Health for the humane treatment of animals.

**Rat Studies.** For microarray analysis, catheters were surgically implanted in the right jugular vein of male Sprague-Dawley rats (9-10 weeks, Harlan Sprague Dawley, Inc. Indianapolis, IN). Twenty-four hours later, rats were given a single intravenous dose of $5.7 \times 10^{12}$ virus particles per kilogram (vp/kg) in a 0.5 ml volume or vehicle alone (phosphate buffered saline, PBS, 0.5 ml). Four days later, animals were sacrificed and the liver immediately excised and stored in RNAlater™ (Qiagen, Valencia, CA) at 4°C for microarray analysis.

**Mouse Studies.** Male C57BL/6 mice (6-8 weeks, Jackson Labs, Bar Harbor, ME) were maintained in a twelve-hour light/dark cycle environment with free access to standard mouse

chow (Harlan, Indianapolis, IN) and deionized water. Following a seven-day acclimation period, a single dose of $1.5 \times 10^{11}$ vp in a volume of 100 µl or vehicle (PBS, 100 µl) was given to mice by tail vein injection. Animals (n = 5 per group) were sacrificed 24 and 48 hours after treatment. At this time, serum was collected and a portion of the liver placed in Tissue-Tek® optimal cutting temperature (O.C.T™) compound (Sakura Finetek, Torrance, CA) for histological analysis. Remaining liver tissues were excised, rinsed in saline, snap frozen in liquid nitrogen and stored at -80°C prior to preparation of microsomes and isolation of nucleic acids for RT-PCR and qRT-PCR.

**Micorarray Evaluation of Hepatic Gene Expression *in vivo*.** The relative expression of genes associated with various signal transduction pathways after virus infection were assessed using oligo GEArray Rat Signal Transduction Pathway Finder microarrays (ORN-014; SuperArray, Frederick, MD). Array grade RNA was isolated using the RNeasy kit (Qiagen, Valencia, CA). Biotin-labeled cDNA probes were synthesized using 3 µg of total isolated RNA and biotin-16-uridine-5′-triphosphate (Roche, Indianapolis, IN) for each array. The membrane was incubated with GEAhyb Hybridization Solution (SuperArray) for 3 hours at 60°C prior to adding 10 µg denatured cDNA probe for overnight hybridization at 60°C. The membrane was then washed twice with 2× saline sodium citrate (SSC) buffer containing 1% sodium dodecyl sulfate (SDS) followed by two additional washes with 0.1× SSC containing 0.5% SDS for 15 minutes each at 60°C. Arrays were blocked with GEArray blocking Solution Q (SuperArray) for 40 minutes at room temperature. Two milliliters of binding buffer (Buffer F, SuperArray), containing a 1:8000 dilution of alkaline phosphatase-conjugated streptavidin (SuperArray), was added for 10 minutes at room temperature. The array image was developed using the CDP-Star chemiluminescent

substrate (SuperArray) and recorded on X-ray film after a 30-minute exposure. The image was scanned using a flatbed scanner (Microtek, Carson, CA).

Arrays were analyzed with ScanAlyze software (Michael Eisen, Lawrence Berkeley National Laboratory) and the GEArray Expression Analysis Suite (SuperArray). Expression levels for each gene on a given array were calculated using minimal background subtraction and interquartile normalization to an internal standard (lactate dehydrogenase A) on each membrane. Data in Table 1 reflect the average ratios of the intensities for a given gene from a given treatment group to that of control animals given saline.

**Histological Analysis of Transgene Expression.** Liver tissues were harvested and immersed in disposable peel-away molds containing Tissue-Tek® O.C.T™ compound and stored at −80°C prior to analysis. Sections were fixed with 0.5% glutaraldehyde (Sigma), and beta-galactosidase activity determined by incubation with the substrate 5-bromo-4-chloro-3-indolyl-beta-galactoside (X-gal, Gold Biotechnology, St Louis, MO) for 4 hours at 37°C in the dark. Staining medium was removed, and blue-colored, positive cells were visually tallied. For GFP analysis, sections of liver tissues were stained with a rabbit anti-GFP antibody (Molecular Probes, Eugene, OR) and with a horseradish-peroxidase (HRP)-conjugated anti-rabbit IgG antibody (Abcam, Cambridge, UK). Spots were developed with 3-amino-9-ethylcarbazole and $H_2O_2$ substrate buffer (Sigma) and counterstained with hematoxylin (Sigma). Tissues were examined with a Lecia DM LB microscope (Leica Microsystems Inc., Buffalo Grove, IL) and photographed using a Leica DFC 320 camera.

**Testosterone Hydroxylation Assay - Microsomes.** Hepatic microsomes were prepared by ultracentrifugation according to established methods (Coon, 1978). Two hundred micrograms of microsomal protein was incubated with testosterone, a NADPH regenerating system (5 mM NADP, 100 mM glucose-6-phosphate, 100 mM magnesium chloride) and 5 units of glucose-6-phosphate dehydrogenase for 15 minutes at 37°C with gentle agitation. The reaction was quenched with dichloromethane and 11α-hydroxyprogesterone added as an internal standard. The organic phase was evaporated under a constant stream of filtered air and samples dissolved in methanol. Testosterone and its metabolites were separated and quantified by high-performance liquid chromatography as described (van der Hoeven, 1984**).** Peak areas of the hydroxylated metabolites were measured and compared to peak areas of the internal standard within the same experimental run.

**Western Blot. Microsomal Proteins:** Hepatic microsomes (50 μg) were separated on 8% (CYP3A) or 12% sodium dodecylsulfate polyacrylamide gels by electrophoresis and transferred to nitrocellulose membranes (BioRad). Protein blots were blocked overnight at 4°C in blocking buffer containing 5% non-fat dry milk in 0.05% (v/v) Tween-20 in Tris buffered saline (TBS-T). After blocking, membranes were incubated with polyclonal rabbit anti-RXR*α* antibody (D20, sc-553), anti-PXR antibody (H-160, sc-25381), or CAR1/2 antibody (M-127, sc-13065), each at a 1:800 dilution, they were then incubated with goat anti-rabbit IgG-HRP secondary antibody (sc-2004, dilution 1:8,000, Santa Cruz Biotechnology, Dallas, TX). To evaluate changes in CYP3A protein, a polyclonal rabbit anti-CYP3A1 antibody (1:3,000 dilution, BD Gentest, Woburn, MA) was used together with a polyclonal anti-rabbit IgG horseradish peroxidase (HRP) conjugated secondary antibody (1:3,000, Cell Signaling Technology, Danvers, MA). **HC-04 cells:** Cells

were washed twice with ice-cold PBS prior to addition of 500 µl of ice-cold lysis buffer (RIPA buffer, Thermo Fisher Scientific, Waltham, MA) containing 1% protease inhibitors (HALT Protease and Phosphatase Inhibitor Cocktail, Pierce, Rockford, IL). After incubation on ice for 5 minutes cells were lysed by extrusion 25 times through a 20-gauge needle (Becton Dickinson, Franklin Lakes, NJ) attached to a 1-ml syringe (Becton Dickinson) and placed on ice for an additional 40 minutes. Lysates were then cleared by centrifugation at 14,000 *g* for 15 minutes at 4°C and stored at −80°C. Proteins (50 µg) were separated on a 12% sodium dodecylsulfate polyacrylamide gel by electrophoresis and transferred to a nitrocellulose membrane (BioRad). Protein blots were blocked overnight at 4°C in blocking buffer containing 3% bovine serum albumin (BSA) in 0.05% TBS-T. Membranes were then incubated for 2 hours with mouse anti-CYP3A4 antibody (1:2000 dilution, HL3, sc-53850) followed by 1 hour of incubation with a goat anti-mouse IgG-HRP antibody (1:10,000 dilution, sc-2005, Santa Cruz Biotechnology). Membranes with siRNA-treated samples were incubated for one hour with the same anti-PXR, anti-CAR and anti-RXR antibodies utilized for microsome blots, each at a 1:800 dilution, followed by 1 hour of incubation with a goat anti-rabbit IgG-HRP antibody (1:10,000 dilution, sc-2004, Santa Cruz Biotechnology). Immune complexes for microsomal proteins and isolated protein from HC-04 cells were detected by chemiluminescence (SuperSignal™ West Pico Chemiluminescene Substrate, Thermo Fisher Scientific). The intensity of protein bands was quantified relative to the signal obtained for an internal standard, β-actin (mouse anti-β-actin monoclonal antibody, AC-15, sc-69879, 1:1000 dilution, Santa Cruz Biotechnology), run on the same gel using Kodak 1D image analysis software (Eastman Kodak Co, Rochester, NY).

DMD Fast Forward. Published on February 11, 2016 as DOI: 10.1124/dmd.115.068874
This article has not been copyedited and formatted. The final version may differ from this version.



**RNA isolation.** RNA was isolated using TRIzol® reagent (Invitrogen, Carlsbad, CA) according to the manufacturer's instructions. Isolated RNA (1 μg) was reverse transcribed with random hexamers using the SuperScript® III first-strand synthesis system (Invitrogen) in a Master Cycler Pro thermal cycler (Eppendorf AG, Hamburg, Germany). Samples were then subject to RT-PCR or qRT-PCR as described below.

**Microsomes (RT-PCR/qRT-PCR).** Changes in CYP3A mRNA expression in mouse liver microsomes were assessed using an AmpliTaq Gold PCR Master Mix kit (Applied Biosystems, Foster City, CA) with the following cycling conditions: 94°C for 30 seconds, 56°C for 30 seconds and 72°C for 1 minute for a total of 32 cycles. Cycling was initiated at 94°C for 3 minutes and terminated at 72°C for 10 minutes. Primer sequences for mouse CYP3A11 were 5′-CTC AAT GGT GTG TAT ATC CCC C-3′ (forward) and 5′-CCG ATG TTC TTA GAC ACT GCC-3′ (reverse) (Xu, 2004). QuantumRNA™ 18S internal standards (Applied Biosystems/Ambion, Austin, TX) using proprietary competimer technology were co-amplified in individual reaction tubes. Reaction products were visualized on a 2% agarose gel containing ethidium bromide and the intensity of each band determined by densitometric analysis using Kodak 1D image analysis software (Eastman Kodak Co). For qRT-PCR PXR, RXRα, and CAR mRNA expression was assessed using SYBR® GreenER™ qPCR SuperMix (Invitrogen) analyzed on a ViiA7™ Real-Time PCR system (Applied Biosystems) with the following cycling conditions: 50°C for 2 minutes, 95°C for 10 minutes followed by 40 cycles of 95°C for 15 seconds and 60°C for 60 seconds. Primer sequences for mouse PXR, RXRα, and CAR were 5′-GTT CAA GGG CGT CAT CAA CT-3′ (forward) and 5′-TTC TGG AAG CCA CCA TTA GG-3′ (reverse); 5′-ACA AGG ACT GCC TGA TCG AC-3′ (forward) and 5′-CAT GTT TGC CTC

CAC GTA TG-3′ (reverse); 5′-CTC AAG GAA AGC AGG GTC AG-3′ (forward) and 5′-AGT TCC TCG GCC CAT ATT CT-3′ (reverse), respectively (Down, 2006).

**Hepatocytes (qRT-PCR).** Changes in gene expression during silencing and virus infection were assessed using a SYBR® Green™ qPCR SuperMix kit (Invitrogen). An aliquot of SuperMix was added to cDNA isolated from HC-04 cells before thermocycling on a ViiA7™ Real-Time PCR system utilizing the same conditions as described above. Primer sequences for human CYP3A4, PXR, RXRα, CAR, integrin αv, integrin β3 and integrin β5 were as follows: 5′-GAT TGA CTC TCA GAA TTC AAA AGA AAC TGA-3′ (forward) and 5′-GGT GAG TGG CCA GTT CAT ACA TAA TG-3′ (reverse) (Yoshitsugu, 2006); 5′-AGA AGG AGA TGA TCA TGT CCG A-3′ (forward) and 5′-GTT TGT AGT TCC AGA CAC TGC C-3′ (reverse) (Gardner-Stephen, 2004); 5′-CCT TTC TCG GTC ATC AGC TC-3′ (forward) and 5′-CTC GCA GCT GTA CAC TCC AT-3′ (reverse) (Lim, 2007); 5′-GCA AGG GTT TCT TCA GGA GAA C-3′ (forward) and 5′-CTT CAC AGC TTC CAG CAA AGG-3′ (reverse) (Tanii, 2013); 5′-AAT CTT CCA ATT GAG GAT ATC AC-3′ (forward) and 5′-AAA ACA GCC AGT AGC AAC AAT-3′ (reverse); 5′-CCG TGA CGA GAT TGA GTC A-3′ (forward) and 5′-AGG ATG GAC TTT CCA CTA GAA-3′ (reverse); 5′-GGA GCC AGA GTG TGG AAA CA-3′ (forward) and 5′-GAA ACT TTG CAA ACT CCC TC-3′ (reverse) (Dingemans, 2010).

All qRT-PCR data was analyzed by the established comparative $C_T$ method using the following equation: Fold change due to treatment = 2^–[($C_T$ gene of interest – $C_T$ internal control) infected animals/cells – ($C_T$ gene of interest – $C_T$ internal control) uninfected animals/cells] (Schmittgen, 2008).

**Serum Cytokines and Transaminases.** Cytokines, IL-6 and IL-12, were quantitated with commercially available ELISA kits according to the manufacturer's protocols (Invitrogen). Serum alanine aminotransferase (ALT) and aspartate aminotransferase (AST) levels were determined using Vitros AST/SGOT and ALT/SGPT DT slides on a Vitros DTSC autoanalyzer (Ortho-Clinical Diagnostics, Rochester, NY).

**Cell culture.** HC-04 cells (human hepatocytes: MRA-975, MR4, ATCC®, Manassas, VA) were maintained in Dulbecco's modified Eagle's medium/Ham's F12 (50/50 ratio, Mediatech, Manassas, VA) supplemented with 10% heat-inactivated fetal bovine serum (Invitrogen) and 2 mM L-glutamine (Hyclone, Logan ,UT).

**RNA interference - HC-04 cells.** HC-04 cells were seeded in either 6 well tissue culture dishes at a density of $1 \times 10^5$ cells per well or in 96 well tissue culture plates (Falcon, Becton Dickinson Labware, Franklin Lakes, NJ) at a density of $6 \times 10^3$ cell per well in complete HC-04 culture medium 48 hours prior to transfection. Cells in each well were then transfected with 100 pmol (6 wells) or 5 pmol (96 wells) of siRNA targeting integrin αv (sc-29373), β3 (sc-29375) and/or β5 (sc-35680) (Santa Cruz Biotechnology) using Lipofectamine 2000 (Invitrogen) according to the manufacturer's instructions. For double silencing studies, 50 pmol (6 wells) or 2.5 pmol (96 wells) of siRNA was used for each target. Efficiency of the knockdown was confirmed by qRT-PCR and compared with expression levels in cells treated with a non-specific siRNA control (sc-37007, Santa Cruz Biotechnology). Forty-eight hours after silencing, cells were infected with either AdlacZ at a multiplicity of infection (MOI) of 500 or an equivalent volume of saline as a

control for 72 hours prior to assessing CYP3A4 activity using a P450-Glo CYP3A4 Luciferin-IPA assay kit (Promega, Madison, WI). Data was generated through comparison of CYP3A4 activity in virus-infected cells to activity in uninfected, saline-treated cells in which the same integrin subunit was silenced. Activity in the uninfected cells was normalized to 100% and data reported as activity which remained after virus infection (% remaining activity). The activity of CYP3A4 in control cells treated with non-specific siRNA was ± 4.65% of the activity of untreated HC-04 cells, which is similar to the range found in a normal human control population (Hirth, 2000).

**Statistical Analysis.** Statistical analysis of data was performed using SigmaStat (Systat Software Inc., San Jose, CA). Differences with respect to treatment were calculated using a one-way analysis of variance followed by a Bonferroni/Dunn *post hoc* test. Differences were determined to be significant when the probability of chance explaining the results was reduced to less than 5% ($p < 0.05$).

## Results

**Hepatic Microarray Analysis of Signal Transduction Pathways After a Single Dose of Adenovirus.** During some of the initial studies conducted in our laboratory in which we characterized CYP3A expression and function in the rat (Callahan, 2005; Callahan, 2006; Callahan, 2008a), samples of liver tissue were taken and processed for assessment of changes in genes associated with different signal transduction patterns. Samples were taken four days after administration of four different live and inactivated recombinant adenovirus vectors to rats: AdlacZ (a first generation E1/E3 deleted adenovirus serotype 5 virus expressing the *E. coli* beta-galactosidase transgene under the control of a CMV promoter), PEGAd (the AdlacZ virus modified by covalent attachment of PEG to the virus capsid which reduces the immune response to the virus (Croyle, 2001; Croyle, 2002)), HDAd (a third-generation adenovirus in which all elements of the viral genome except the inverted terminal repeats (ITRs) and the packaging signal (Ψ) are removed and which also contains the beta-galactosidase transgene (Croyle, 2005)) and UVAd (the AdlacZ vector inactivated by exposure to UV light (Callahan, 2008b)). Data from these samples were compared to saline-treated controls (Vehicle). Significant increases in gene expression in adenovirus-treated samples are summarized in Table 1. Figure 1 shows representative microarray images on which five signal transduction pathways linked to CYP3A expression are highlighted. These were consistently upregulated in all virus-treated animals. Two genes associated with the NFκB pathway, B-cell leukemia/lymphoma2 related protein A1 (Bcl2a1) and nuclear factor kappa light chain gene enhancer in B-cells 1 (Nfkb1), were significantly altered by all of the vectors. Levels of Bcl2a1 were increased 1.8, 6.5, 15.4, and 2.8-fold following AdlacZ, PEGAd, HDAd, and UVAd treatment, respectively. Nfkb1 was increased by a factor of 1.8, 3.5, 3.8, and 1.4 after treatment with AdlacZ, PEGAd, HDAd, and UVAd.

Two genes involved in the protein kinase C (PKC) pathway, c-Jun N-terminal kinase (JNK/Jun) and ornithine decarboxylase 1 (Odc1), were increased in the AdlacZ group (3.4 and 3.5-fold) and PEGAd (5.6 and 2.8-fold). Odc1 was elevated 4.3-fold in HDAd-treated animals and Jun was increased 2.7-fold following UVAd treatment. Administration of the HDAd vector caused the largest induction, 7.9-fold, in the expression of monokine induced by IFN-gamma (Mig), a gene associated with the Jak-Stat pathway. Another gene associated with the Jak-Stat pathway, interferon regulatory factor 1 (Irf1), was elevated 2.4, 4.1, 3.2, and 2.3-fold in AdlacZ, HDAd, and UVAd-treated animals when compared to saline treated control animals. Expression of cyclin D1 (Cend1) and phosphatase and tensin homolog (Pten), two genes associated with the PI3K signaling pathways, resulted in the largest increase after PEGAd administration (6.5-fold) and HDAd-treatment (8.5-fold), respectively. The last highlighted pathway is the retinoic acid pathway where expression of cathepsin D (Ctsd) was increased by a factor if 1.5, 4.1, and 3.0 in AdlacZ, PEGAd, and UVAd-treated animals, receptively. Another gene associated with this pathway, retinol binding protein 1, cellular (Rbp1), was induced 1.4, 2.2, 1.9, and 2.3-fold following treatment with AdlacZ, PEGAd, HDAd and UVAd, respectively. These results in conjunction with *in vitro* studies in which CYP3A was suppressed after treatment with a peptide rich in RGD sequences, known to engage integrin receptors (Campbell, 2011), served as the basis for the studies outlined in this manuscript.

**Effect of Integrin-Independent Virus Infection on Hepatic CYP3A Expression and Function *in vivo*.** To date, all of our studies evaluating the expression and function of hepatic CYP3A during adenovirus infection were conducted in the rat model. The *in vivo* experiments summarized below were conducted in the mouse model so that if a connection between integrin

silencing/engagement and CYP3A expression was made *in vivo*, additional mechanistic experiments could be conducted in knockout models with similar backgrounds. Thus, to validate our hypothesis that virus-integrin interactions are required for infection-induced changes in CYP3A *in vivo*, mice were given a single dose of either AdlacZ or a similar virus in which the RGD motif within the penton capsid protein was deleted via PCR-directed mutagenesis (AdΔRGD, Shayakhmetov, 2005a). Twenty-four hours after administration, mice given the AdlacZ vector experienced a notable reduction in CYP3A catalytic activity, approximately 70% compared to saline-treated mice (PBS, Figure 2A, $p < 0.01$). Forty-eight hours after treatment, CYP3A activity continued to be suppressed in the AdlacZ group (56.4% of control, Figure 2B, $p < 0.01$). Conversely, the AdΔRGD vector did not alter CYP3A activity at either timepoint. A similar trend was noted with respect to CYP3A protein expression with reductions of 38% and 23% of control noted 24 and 48 hours after administration of AdlacZ respectively (Figure 2C and 2D, $p < 0.05$) while protein levels were unaltered by the AdΔRGD virus. CYP3A11 mRNA levels were also reduced by the AdlacZ vector (32.8% of control) 24 hours after treatment (Figure 2E, $p < 0.05$) and returned to baseline levels 48 hours after infection (Figure 2F, $p = 0.67$). CYP3A11 mRNA levels were unaffected by AdΔRGD throughout the study period. The observation that CYP3A activity was suppressed to a greater extent than protein and gene expression after infection with AdlacZ is not unique to these studies as it has previously been seen *in vitro* and could be due to posttranslational modifications of the CYP3A enzyme (Wonganan, 2014).

**Histochemical Evaluation of Transgene Expression.** In order to determine that differences in CYP3A expression between the AdlacZ and the AdΔRGD virus were not simply due to

disparities in the ability of each virus to infect the liver, tissue sections from mice given the AdlacZ vector were stained with the histochemical substrate for the beta-galactosidase transgene, X-gal, while livers from mice given AdΔRGD were stained with an antibody against the green fluorescent protein transgene (GFP, Figure 3). Staining of tissues obtained from animals given a saline bolus (vehicle, negative control) revealed minimal endogenous levels of either transgene in the liver (Figures 3A, 3E, and 3I). Twenty-four hours after administration of AdlacZ, approximately 80% of the cells were positive for beta-galactosidase (Figure 3B), while 15% of the cells in sections taken from mice given AdΔRGD were positive for GFP (Figure 3G). GFP expression increased in these animals at the 48 hour timepoint with approximately 80% of hepatocytes expressing the transgene (Figure 3K). Sections from animals given an adenovirus expressing GFP without the RGD mutation demonstrated similar transgene expression patterns at 24 and 48 hours (Figures 3H and 3L). Endogenous staining for beta-galactosidase was not present in any of the sections obtained from animals given viruses expressing GFP (Figures 3C and 3D.) GFP was also absent in sections obtained from animals given AdlacZ (Figures 3F and 3J).

**Effect of Integrin-Independent Entry on the Toxicology Profile of Recombinant Adenovirus.** Cytokines IL-6 and IL-12 were selected for evaluation in our studies since IL-6 is a hallmark indicator of macrophage activation and IL-12 that of dendritic cell activation in response to adenovirus infection (Schnell, 2001; Zhang, 2001). In each of these antigen presenting cells, integrins are required for transcription and for functional activation of each cytokine protein via the endosomal escape pathway (Di Paolo, 2009). In a manner that has been noted previously in our laboratory and those of others, serum IL-6 was significantly elevated 6

hours after administration of the AdlacZ vector (1,105 ± 226.1 pg/ml, Figure 4A). IL-6 levels were significantly lower in samples taken from animals given AdΔRGD at the same timepoint (340.4 ± 50.1 pg/ml). IL-6 declined to 38.2 ± 11.7 pg/ml by 24 hours after infection with AdlacZ. It was not detectable in samples taken from animals given AdΔRGD at this timepoint and in any sample collected 48 hours after treatment. The IL-12 profile for AdlacZ was similar to that for IL-6 in that levels spiked to 1,175.7 ± 103.1 pg/ml at 6 hours and declined to 109.2 ± 28.6 and 25.6 ± 17.9 pg/ml at the 24 and 48 hour timepoints respectively (Figure 4B). IL-12 in samples obtained 6 hours after administration of AdΔRGD was 3 times lower than those from mice given AdlacZ (392.1 ± 26.1 pg/ml), however, the concentration of this cytokine was significantly higher than that detected in the AdlacZ group at the 24 hour (247.6 ± 30.3 pg/ml) and 48 hour (270.0 ± 18.6 pg/ml) timepoints. This finding was somewhat unexpected, however, early studies with AdΔRGD and the native wild-type virus described notable differences in intracellular trafficking and endosomal escape patterns (Shayakhmetov, 2005a), processes which significantly impact development of the innate immune response to the virus (Leopold, 2007; Teigler, 2014). Other studies in which AdΔRGD was given to mice in the same manner as described in our studies have reported notable suppression of a variety of pro-inflammatory cytokines (Di Paolo, 2009), however, levels of cytokines with dual inflammatory and protective roles after administration of the virus have not previously been described. When looking at the IL-6 data, it is clear that the inability of AdΔRGD to stimulate the cells through an integrin-dependent pathway suppressed production of this cytokine. In contrast, integrin-independent interaction of the virus with dendritic cells induced production of IL-12 in a potentially inactive form and/or in a form incapable of escalating the immune response to this modified virus (Zundler, 2015).

DMD Fast Forward. Published on February 11, 2016 as DOI: 10.1124/dmd.115.068874
This article has not been copyedited and formatted. The final version may differ from this version.



Serum aspartate aminotransferase (AST) and alanine aminotransferase (ALT) levels are often used as indicators for determining liver function during inflammation, injury, or disease (Ozer, 2008). Twenty-four hours following virus administration, AST levels were 4 (AdlacZ) and 3 (AdΔRGD) times that of saline-treated animals (Figure 4C). At this time, serum ALT was also 9 and 5 times above baseline in samples from mice given the AdlacZ and AdΔRGD vectors respectively (Figure 4D). At the 48 hour timepoint, serum AST levels in mice given the AdΔRGD vector were not significantly different from those given saline (127.7 $\pm$ 5.2 vs. 85.7 $\pm$ 20.9 $p = 0.18$), while those from mice given AdlacZ were still notably elevated (193.3 $\pm$ 27.1 U/L, Figure 4E). ALT levels were still significantly higher than baseline in samples taken from each treatment group at the 48-hour timepoint (Figure 4F, $p < 0.05$).

**Effect of Integrin-Independent Entry on Nuclear Receptors Regulating CYP3A Expression.** On a transcriptional level, hepatic CYP3A is constitutively expressed in the liver but several nuclear receptors, including the pregnane X receptor (PXR), constitutive androstane receptor (CAR), and retinoid X receptor (RXR) are primarily responsible for regulating CYP3A gene expression (Croyle, 2009). However, it remains to be known which is predominantly influenced by virus infection and ultimately responsible for our observed changes in CYP3A (Callahan, 2008a; Wonganan, 2014). In an effort to determine how integrin engagement changes each of these key regulators of CYP3A *in vivo*, gene and protein expression was determined 24 and 48 hours after infection with each virus (Figure 5). PXR gene expression was unaffected by AdlacZ 24 and 48 hours after infection. In contrast, a 2-fold increase was seen at 24 hours and a 2-fold decrease observed at 48 hours after infection with AdΔRGD with respect to uninfected saline

controls (Figure 5A). PXR protein levels increased 24 hours after administration of both viruses and declined to baseline (AdΔRGD) and below baseline (AdlacZ) levels at 48 hours (Figure 5B, $p < 0.05$ and $p < 0.01$). RXRα gene expression was unaffected for animals treated with AdΔRGD for 24 and 48 hours. However samples collected 48 hours after AdlacZ infection showed a 5-fold reduction in RXRα mRNA (Figure 5C). RXRα protein expression was reduced 27% (24 hours) and 63% (48 hours) for AdlacZ-infected animals with respect to saline controls (Figure 5D, $p < 0.05$ and $p < 0.01$). A 2-fold reduction was seen in CAR gene expression in animals treated with AdlacZ for 24 and 48 hours while treatment with AdΔRGD did not have any effect on this nuclear receptor (Figure 5E). A general trend of suppressed protein levels was observed for CAR in animals infected with either virus (Figure 5F, $p < 0.01$).

**Treatment with an Integrin-Specific Peptide Inhibits CYP3A4 Activity in the HC-04 Cell Line.** To confirm that a human hepatic cell line (HC-04) can be used for mechanistic studies involving virus-integrin and CYP3A interactions, an initial pilot experiment was performed in which HC-04 cells were treated with a linear peptide containing a RGD sequence, a known integrin receptor ligand, or control RGE (arginine-glycine-glutamic acid, 1.5 mg/ml) peptide that does not engage integrins. Treatment with the RGD peptide significantly suppressed CYP3A4 activity in HC-04 cells by 40% with respect to untreated controls while the RGE peptide did not effect CYP3A catalytic activity (Figure 6A) in the absence of virus infection. The amount of peptide used was sufficient to cover the majority of integrin receptors on the cells as, in a separate experiment, it reduced the transduction efficiency of AdlacZ by approximately 70% (Figures 6B and 6C). Results from this study confirm results from previous studies performed in primary rat hepatocytes (Callahan, 2008a), making this cell line useful for further mechanistic

studies to determine how integrins regulate CYP3A4 in humans.

**Impact of Silencing of Integrin Expression on the Catalytic Activity of Hepatic CYP3A4 *in vitro.*** To determine which components of the integrin receptor that regulate CYP3A4, expression of αv, β3 and/or β5 subunits were knocked down via siRNA targeting in the HC-04 cell line. Forty-eight hours after transfection with optimized sequences, gene expression was confirmed to be reduced by 3.5 fold for integrin αv and β3, and 4 fold for integrin β5 (Figure 7A). When silencing both subunits at the same time, the αvβ3 combination allowed for the most maximal suppression (3.6 fold below cells transfected with a non-targeting siRNA sequence, Figure 7A). At this time (48 hours post-silencing), cells were infected with virus (AdlacZ, MOI 500) or saline and, 72 hours later, CYP3A4 activity was assessed. Adenovirus-mediated suppression of CYP3A4 activity was still seen in cells treated with negative control siRNA and αv siRNA (reduced by 70% and 75% with respect to uninfected controls respectively, Figure 7B). Very minimal reductions in CYP3A4 activity were detected when the β3 or β5 subunit was silenced (7% and 23% reduction, respectively). Less of an effect (6-10% reduction) was seen when both αv and β subunits were silenced together (Figure 7B).

**Silencing of Integrin Subunits Alters CAR and PXR Gene Expression *in vitro.*** Baseline gene and protein expression levels of the nuclear receptors PXR, CAR and RXRα was determined in HC-04 cells 48 hours after knockdown of each integrin subunit (Figure 8). Silencing of subunits αv and β3 decreased gene expression of PXR by 6- and 5-fold, respectively, while silencing of the β5 subunit had no effect (Figure 8A). A general trend of reduction in PXR protein expression after integrins were silenced was observed, however, this was not found to be

statistically significant (Figure 8B). Silencing of either β-subunit significantly decreased gene and protein expression level of CAR while silencing of the αv subunit did not alter CAR at the mRNA or protein level (Figure 8C and 8D, respectively). Silencing with either αv, β3 or β5 siRNA had no significant effect on RXRα, although the general trend was a small increase in the gene expression level of RXRα when silencing the αv and β5 subunits (Figure 8E). RXRα protein levels were not affected by silencing of any of the integrin receptor subunits (Figure 8F).

## Discussion

Like many other pathogens, human adenovirus serotype 5 utilizes additional receptors like the coxsackie- and adenovirus receptor (AdCAR) and heparan sulfate proteoglycans (HSPGs) to enter cells (Arnberg, 2012). While integrins facilitate internalization of virus particles, AdCAR and HSPGs are responsible for viral attachment to the hepatocyte (Wolfrum, 2013). Until recently, HSPGs were considered to be the primary hepatic receptor for adenovirus binding *in vivo* (Kalyuzhniy, 2008; Zaiss, 2015). However, studies in knockout mice suggest that the LDL receptor-related protein (LRP), may be responsible for adenovirus-mediated transduction of human liver and in various animal models of disease (Shayakhmetov, 2005b; Zaiss, 2015). AdCAR is poorly expressed in the liver *in vivo* but has been shown to mediate infection in cultured cells (Zaiss, 2015). AdΔRGD transduced the liver of mice in the outlined studies through these alternative receptors. The role of these receptors in the regulation of CYP3A seems minimal since our data clearly shows that elimination of the adenovirus-integrin interaction reverses virus-induced changes in CYP previously noted with wild type virus.

Integrins lack intrinsic enzymatic signaling, instead, they are activated by binding of extracellular ligands (like viruses and other microbes), which results in clustering and changes in ligand-binding affinity of integrins on the cell surface (Goodman, 2012). Activation in this manner also changes the tertiary and quaternary structures of these receptors, which propagate across the cell membrane to activate cytoplasmic kinase- and cytoskeletal-signaling cascades. This outside-in response, initiates changes in cell polarity, survival, proliferation, cytoskeletal structure and gene expression (Campbell, 2011). Integrins are also regulated by internal stimuli, initiating intracellular signals, which convert the extracellular domains into a high-affinity

ligand-binding state. This inside-out response (Ye, 2011), affects cell adhesion, migration and extracellular matrix assembly (Goodman, 2012). Given that adenovirus infection is a complex, multistage process, we believe that the virus induces a sustained effect on CYP3A expression and function by first inducing pathways stimulated by the outside-in response during internalization followed by induction of additional pathways stimulated by the inside-out response during nuclear transit and expression of virus genes throughout the cell. We also realize that, while simple engagement of integrins with the RGD peptide elicited a comparable reduction in CYP3A activity to that seen with adenovirus, this effect may be induced by a different mechanism as monomeric RGD-peptides are internalized via a fluid-phase endocytic pathway (Sancey, 2009). Additional *in vitro* and *in vivo* studies with RGD-based integrin ligands and other integrin and non-integrin dependent pathogens are currently underway in our laboratory to further define the role of the outside-in and the inside-out response on hepatic CYP3A expression and to confirm that our observations are not unique to the adenovirus.

The most interesting finding of these studies was that silencing of the β3- and β5- integrin subunits reversed the effect of adenovirus-mediated suppression of CYP3A4 in human hepatocytes (Figure 7). This is important since the β subunit is largely responsible for the inside-out response. The key activator of the inside-out response is the intracellular protein talin. Talin binds specifically to the tail of the β-subunit of the integrin receptor (Calderwood, 1999) resulting in separation of the α- and β-tail ultimately leading to increased binding affinity of the integrin receptor (Morse, 2014). Several viral proteins interact with talin *in vivo* in various acts of self-preservation (Brown, 2011; Stanton, 2014). Disruption of the β-subunit and talin interaction by pUL135 protein suppresses integrin function and protects human cytomegalovirus

from natural killer and T cells (Stanton, 2014). In contrast, knockdown of talin enhances susceptibility to retroviral infection in human cells (Brown, 2011). To date, adenovirus-talin interactions have not been described. Hence, *in vitro* studies in which talin is silenced and *in vivo* studies utilizing talin knockout animal models (Calderwood, 2013) should be preformed to determine what role talin plays in the regulation of CYP3A4.

Nuclear receptors, including the pregnane X receptor (PXR), constitutive androstane receptor (CAR), and retinoid X receptor (RXR), are primarily responsible for regulating hepatic CYP3A expression (Croyle, 2009). Analysis of changes in each of these receptors *in vivo* revealed that RXRα, essential for binding of nuclear receptors to the dXREM and prPXRE regions of the CYP3A4 5' promoter (Wang, 2008), was involved in the observed downregulation of CYP3A via integrin-virus interactions (Figure 5). This observation was not congruent with those made in cultured human hepatocytes where RXRα gene and protein expression was not significantly affected by silencing of β integrins (Figure 8). An interesting biphasic response of PXR was induced *in vivo* by both viruses, indicating that it was affected in an integrin-independent manner. Silencing experiments did not reflect these observations as PXR was notably suppressed when the β3 integrin subunit was silenced. It is not clear at this time if these disparities are due to species-specific differences or differences in inside-out/outside-in responses between *in vivo* and *in vitro* systems. Studies using both the AdlacZ- and AdΔRGD viruses in RXRα and PXR knockout mice, primary hepatocytes isolated from these animals and human hepatocytes in which each nuclear receptor is silenced will assist us in making these distinctions. While notable reductions in CAR were observed in animals given AdlacZ only, they were less profound than RXRα, suggesting that CAR is less responsive to virus-induced changes in CYP3A initiated

through integrin engagement. In contrast CAR was more responsive to silencing of integrins, especially the β subunits, than RXRα (Figure 8). This suggests that β3 holds its influence over CYP3A by downregulating PXR and CAR.

While silencing of integrin subunits clearly influenced CYP3A activity and mRNA levels of nuclear receptors, protein levels of each remained largely unaffected. This coupled with the fact that CYP3A activity was suppressed to a greater extent than protein and mRNA levels in our *in vivo* studies suggests that post-translational modification of CYP3A and/or various nuclear receptors may be responsible for integrin-induced changes in hepatic CYP3A (Figure 2). Microarray studies conducted early in our assessment of how CYP3A responds to adenovirus infection (Figure 1, Table 1) demonstrated that several signal transduction pathways known to phosphorylate RXR, PXR and CAR and alter formation of transcriptional complexes to drive CYP3A expression (Shao, 1999; Brandlin, 2002; Pimienta, 2007) were upregulated in the liver. These pathways and others initiated by the engagement of integrin receptors may also alter CYP3A in a similar manner. Data in Figure 8 also suggests that specific integrin subunits may uniquely impact CYP3A activity and expression through different mechanisms/pathways. We are currently developing assays for studying changes in posttranslational modifications of CYP3A4, CAR, PXR, and RXRα during virus infection using mass spectrometry. These assays paired with evaluation of promoter occupancy by each nuclear receptor during virus infection will be paramount to further study the role of each integrin subunit on hepatic CYP3A expression and function in the future.

Integrin receptors have been implicated in the regulation of several functions in tumor cells such as migration, invasion, proliferation and survival. The diversity in these processes suggests that pathology of cancer, as well as other non-infectious diseases in which integrins play a role such as cardiovascular disease, diabetes and wound healing, may not be attributed to a single integrin receptor, but instead are the end result of crosstalk between several integrin receptors. Thus, drugs targeting single as well as multiple integrin receptors have been developed for treatment of cancer and other diseases (Desgrosellier, 2010; Sheldrake, 2014). In this context, data generated in our studies suggest that hepatic drug metabolism patterns can be significantly altered in response to these medications which will most likely be given with other chemotherapeutic agents that are metabolized by CYP3A4; either resulting in an enhanced therapeutic effect or severe toxicities due to accumulation of unmetabolized by-products over time. Various expression patterns of integrins have been shown to correlate with increased tumor progression and decreased patient survival in breast, cervical and colon cancers (Desgrosellier, 2010). Recent findings have shown that cancer cells change their integrin repertoire in response to drug treatment (Sheldrake, 2014). Given the link between integrin expression and CYP3A4 activity illustrated here, integrin receptors may play a notable role in the development of drug resistance. Experiments to further explore the correlation between integrin expression, CYP3A4 activity and tumor resistance are underway in our laboratory. Understanding this interplay could potentially be used to regulate integrin expression during the early stages of cancer development to mitigate severity of disease or to modulate drug metabolism to improve therapeutic outcomes in patients through personalized drug therapies directed at integrins.

We have shown, for the first time, a direct correlation between engagement of integrin receptors

and the regulation of hepatic CYP3A activity. Although engagement of other intracellular receptors including Toll-like receptors (TLRs) have been implicated in the regulation of CYP3A during infection (Shah, 2014), we now provide evidence supporting the notion that extracellular receptors influence hepatic drug metabolism under infectious and non-infectious conditions. These results may translate beyond CYP3A activity as several nuclear receptors that regulate it play notable roles in the regulation of other metabolic enzymes and drug transporters. We are currently assessing the function of several hepatic efflux and uptake transporters *in vivo* and *in vitro* in response to integrin expression.

## Acknowledgements

We thank MR4 for providing us with HC-04 cells contributed by Jetsumon Sattabongkot Prachumsri and Dr. Dmitry Shayakhmetov (Emory University) for kindly providing the AdΔRGD construct. We also thank Dahlia Astone and Dr. Lucio Pastore of The University of Naples, Federico II for assistance in establishing the helper-dependent adenovirus system in our laboratory. We would also like to acknowledge the expert technical assistance of Mr. Stephen C. Schafer in the preparation of histochemical images depicted in this manuscript.

## Authorship Contributions

Participated in research design: Jonsson-Schmunk, Wonganan, Choi, Callahan and Croyle

Conducted experiments: Jonsson-Schmunk, Wonganan, Choi and Callahan

Performed data analysis: Jonsson-Schmunk, Wonganan, Choi, Callahan and Croyle

Wrote or contributed to the writing of the manuscript: Jonsson-Schmunk, Wonganan, Choi and Croyle

## References

Arnberg N (2012) Adenovirus receptors: implications for targeting of viral vectors. *Trends Pharmacol Sci* **33:**442-448.

Brandlin I, Eiseler T, Salowsky R, Johannes FJ (2002) Protein kinase C(mu) regulation of the JNK pathway is triggered via phosphoinositide-dependent kinase 1 and protein kinase C(epsioln). *J Biol Chem* **277:**45451-45457.

Brown C, Morham SG, Walsh, D, Naghavi MH (2011) Focal adhesion proteins talin-1 and vinculin negatively affect paxillin phosphorylation and limit retroviral infection. *J Mol Biol* **410:**761-777.

Calderwood D, Campbell ID, Critchley DR (2013) Talins and kindlins: partners in integrin-mediated adhesion. *Nat Rev Mol Cell Biol* **14:**503-517.

Calderwood D, Zent R, Grant R, Rees DJ, Hynes RO, Ginsberg MH (1999) The Talin head domain binds to integrin beta subunit cytoplasmic tails and regulates integrin activation. *J Biol Chem* **274:**28071-28074.

Callahan S, Boquet MP, Ming X, Brunner LJ, Croyle MA (2006) Impact of transgene expression on drug metabolism following systemic adenoviral vector administration. *J Gene Med* **8:**566-576.

Callahan S, Ming X, Lu SK, Brunner LJ, Croyle MA (2005) Considerations for use of recombinant adenoviral vectors: dose effect on hepatic cytochromes P450. *J Pharmacol Exp Ther* **312:**492-501.

Callahan S, Wonganan P, Croyle MA (2008a) Molecular and macromolecular alterations of recombinant adenoviral vectors do not resolve changes in hepatic drug metabolism during infection. *Virol J* **30:**111.

Callahan S, Wonganan P, Obenauer-Kutner LJ, Sutjipto S, Dekker JD, Croyle MA (2008b) Controlled inactivation of recombinant viruses with vitamin B2. *J Virol Methods* **148:**132-145.

Campbell I, Humphries MJ (2011) Integrin structure, activation, and interactions. *Cold Spring Harb Perspect Biol* **3:**a004994.

Caswell P, Vadrevu S, Norman JC (2009) Integrins: masters and slaves of endocytic transport. *Nat Rev Mol Cell Biol* **10:**843-853.

Coon M, van der Hoeven TA, Dahl SB, Haugen DA (1978) Two forms of liver microsomal cytochrome P450, P-450lm2 and P450LM4 (rabbit liver). *Methods Enzymol* **52:**109-117.

Cox D, Brennan M, Moran N (2010) Integrins as therapeutic targets: lessons and opportunities. *Nat Rev Drug Discov* **9:**804-820.

Croyle M (2009) Long-term virus-induced alterations of CYP3A-mediated drug metabolism: a look at the virology, immunology and molecular biology of a multi-faceted problem. *Expert Opin Drug Metab Toxicol* **5:**1189-1211.

Croyle M, Chirmule N, Zhang Y, Wilson JM (2002) PEGylation of E1-deleted adenovirus vectors allows significant gene expression on readministration to liver. *Hum Gene Ther* **13:**887-900.

Croyle M, Chirmule N, Zhang Y, Wilson JM (2001) "Stealth" adenoviruses blunt cell-mediated and humoral immune responses against the virus and allow for significant gene expression upon readministration in the lung. *J Virol* **75:**4792-4801.

Croyle M, Le HT, Linse KD, Cerullo V, Toietta G, Beaudet A, Pastore L (2005) PEGylated helper-dependent adenoviral vectors: highly efficient vectors with an enhanced safety profile. *Gene Ther* **12:**579-587.

Croyle M, Yu QC, Wilson JM (2000) Development of a rapid method for the PEGylation of adenoviruses with enhanced transduction and improved stability under harsh storage conditions. *Hum Gene Ther* **11:**1713–1722.

Desgrosellier J, Cheresh DA (2010) Integrins in cancer: biological implications and therapeutic opportunities. *Nat Rev Cancer* **10:**9-22.

Di Paolo N, Miao EA, Iwakura Y, Murali-Krishna K, Aderem A, Flavell RA, Papayannopoulou T, Shayakhmetov DM (2009) Virus binding to a plasma membrane receptor triggers interleukin-1 alpha-mediated proinflammatory macrophage response in vivo. *Immunity* **31:**110-121.

Ding X, Staudinger JL (2005) Repression of PXR-mediated induction of hepatic CYP3A gene expression by protein kinase C. *Biochem Pharmacol* **69:**867-873.

Dingemans A, van den Boogaart V, Vosse BA, van Suylen RJ, Griffioen AW, Thijssen VL (2010) Integrin expression profiling identifies integrin alpha5 and beta1 as prognostic factors in early stage non-small cell lung cancer. *Mol Cancer* **17:**152.

Down M, Arkle S, Mills JJ (2006) Regulation and induction of CYP3A11, CYP3A13 and CYP3A25 in C57BL/6J mouse liver. *Arch Biochem Biophys* **457:**105-110.

Forsyth C, Plow EF, Zhang L (1998) Interaction of the fungal pathogen Candida albicans with integrin CD11b/CD18: recognition by the I domain is modulated by the lectin-like domain and the CD18 subunit. *J Immunol* **161:**6198-6205.

Gandhi A, Moorthy B, Ghose R (2012) Drug disposition in pathophysiological conditions. *Curr Drug Metab* **13:**1327-1344.

Gardner-Stephen D, Heydel JM, Goyal A, Lu Y, Xie W, Lindblom T, Mackenzie P, Radominska-Pandya A (2004) Human PXR variants and their differential effects on the regulation of human UDP-glucuronosyltransferase gene expression. *Drug Metab Dispos* **32:**340-347.

Goodman S, Picard M (2012) Integrins as therapeutic targets. *Trends Pharmacol Sci* **33:**405-412.
Hauck C, Borisova M, Muenzner P (2012) Exploitation of integrin function by pathogenic microbes. *Curr Opin Cell Biol* **24:**637-644.

Hirth J, Watkins PB, Strawderman M, Schott A, Bruno R, Baker LH (2000) The effect of an individual's cytochrome CYP3A4 activity on docetaxel clearance. *Clin Cancer Res* **6:**12551258.

Kacevska M, Mahns A, Sharma R, Clarke SJ, Robertson GR, Liddle C (2013) Extra-hepatic cancer represses hepatic drug metabolism via interleukin (IL)-6 signalling. *Pharm Res* **30:**2270-2278.

Kalyuzhniy O, Di Paolo NC, Silvestry M, Hofherr SE, Barry MA, Stewart PL, Shayakhmetov DM (2008) Adenovirus serotype 5 hexon is critical for virus infection of hepatocytes in vivo. *Proc Natl Acad Sci U S A* **105:**5483-5488.

Leopold P, Crystal RG (2007) Intracellular trafficking of adenovirus: many means to many ends. *Adv Drug Deliv Rev* **59:**810-821.

Lim P, Tan W, Latchoumycandane C, Mok WC, Khoo YM, Lee HS, Sattabongkot J, Beerheide W, Lim SG, Tan TM, Boelsterli UA (2007) Molecular and functional characterization of drug-metabolizing enzymes and transporter expression in the novel spontaneously immortalized human hepatocyte line HC-04. *Toxicol In Vitro* **21:**1390-1401.

Maizel JJ, White DO, Scharff MD (1968) The polypeptides of adenovirus. I. Evidence for multiple protein components in the virion and a comparison of types 2, 7A, and 12. *Virology* **36:**115-125.

Morse E, Brahme NN, Calderwood DA (2014) Integrin cytoplasmic tail interactions. *Biochemistry* **53:**810-820.

Ozer J, Ratner M, Shaw M, Bailey W, Schomaker S (2008) The current state of serum biomarkers of hepatotoxicity. *Toxicology* **245:**194-205.

Pimienta G, Ficarro SB, Gutierrez GJ, Bhoumik A, Peters EC, Ronai Z, Pascual J (2007) Autophosphorylation properties of inactive and active JNK2. *Cell Cycle* **6:**1762-1771.

Pondugula S, Dong H, Chen T (2009) Phosphorylation and protein-protein interactions in PXR-mediated CYP3A repression. *Expert Opin Drug Metab Toxicol* **5:**861-873.

Reiss W, Piscitelli SC (1998) Drug-cytokine interactions: mechanisms and clinical implications. *BioDrugs* **9:**389-395.

Sancey L, Garanger E, Foillard S, Schoehn G, Hurbin A, Albiges-Rizo C, Boturyn D, Souchier C, Grichine A, Dumy P, Coll JL (2009) Clustering and internalization of integrin alphavbeta3 with a tetrameric RGD-synthetic peptide. *Mol Ther* **17:**837-843.

Schmittgen T, Livak KJ (2008) Analyzing real-time PCR data by the comparative C(T) method. *Nat Protoc* **3:**1101-1108.

Schnell M, Zhang Y, Tazelaar J, Gao GP, Yu QC, Qian R, Chen SJ, Varnavski AN, LeClair C, Raper SE, Wilson JM (2001) Activation of innate immunity in nonhuman primates following intraportal administration of adenoviral vectors. *Mol Ther* **3:**708-722.

Sevior D, Pelkonen O, Ahokas JT (2012) Hepatocytes: the powerhouse of biotransformation. *Int J Biochem Cell Biol* **44:**257-261.

Shah P, Guo T, Moore DD, Ghose R (2014) Role of constitutive androstane receptor in Toll-like receptor-mediated regulation of gene expression of hepatic drug-metabolizing enzymes and transporters. *Drug Metab Dispos* **42:**172-181.

Shao D, Lazar MA (1999) Modulating nucelar receptor function: may the phos be with you. *J Clin Invest* **103:**1617-1618.

Shattil S, Kim C, Ginsberg MH (2010) The final steps of integrin activation: the end game. *Nat Rev Mol Cell Biol* **11:**288-300.

Shayakhmetov D, Eberly AM, Li Z-Y, Lieber A (2005a) Deletion of penton RGD motifs affects the efficiency of both the internalization and the endosome escape of viral particles containing adenovirus serotype 5 or 35 fiber knobs. *J Virol* **79:**1053-1061.

Shayakhmetov D, Gaggar A, Ni S, Li ZY, Lieber A (2005b) Adenovirus binding to blood factors results in liver cell infection and hepatotoxicity. *J Virol* **79:**7478-7491.

Sheldrake H, Patterson LH (2014) Strategies to inhibit tumor associated integrin receptors: rationale for dual and multi-antagonists. *J Med Chem* **57:**6301-6315.

Stanton R, Prod'homme V, Purbhoo MA, Moore M, Aicheler RJ, Heinzmann M, Bailer SM, Haas J, Antrobus R, Weekes MP, Lehner PJ, Vojtesek B, Miners KL, Man S, Wilkie GS, Davison AJ, Wang EC, Tomasec P, Wilkinson GW (2014) HCMV pUL135 remodels the actin cytoskeleton to impair immune recognition of infected cells. *Cell Host Microbe* **16:**201-214.

Stewart P, Nemerow GR (2007) Cell integrins: commonly used receptors for diverse viral pathogens. *Trends Microbiol* **15:**500-507.

Tanii H, Shitara Y, Torii M, Sekine S, Iwata H, Horie T (2013) Induction of cytochrome P450 2A6 by bilirubin in human hepatocytes. *Pharmacol Pharm* **4:**182-190.

Teigler J, Kagan JC, Barouch DH (2014) Late endosomal trafficking of alternative serotype adenovirus vaccine vectors augments antiviral innate immunity *J Virol* **88:**10354-10363.

van der Hoeven T (1984) Assay of hepatic microsomal testosterone hydroxylases by high-performance liquid chromatography. *Anal Biochem* **138:**57-65.

Wang K, Chen S, Xie W, Wan YJ (2008) Retinoids induce cytochrome P450 3A4 through RXR/VDR-mediated pathway. *Biochem Pharmacol* **75:**2204-2213.

Wolfrum N, Greber UF (2013) Adenovirus signalling in entry. *Cell Microbiol* **15:**53-62.

Wonganan P, Jonsson-Schmunk K, Callahan SM, Choi JH, Croyle MA (2014) Evaluation of the HC-04 cell line as an in vitro model for mechanistic assessment of changes in hepatic cytochrome P450 3A during adenovirus infection. *Drug Metab Dispos* **42:**1191-1201.

Xu D, Wei W, Sun MF, Wu CY, Wang JP, Wei LZ, Zhou CF (2004) Kupffer cells and reactive oxygen species partially mediate lipopolysaccharide-induced downregulation of nuclear receptor pregnane x receptor and its target gene CYP3a in mouse liver. *Free Radic Biol Med* **37:**10-22.

Ye F, Kim C, Ginsberg MH (2011) Molecular mechanism of inside-out integrin regulation. *J Thromb Haemost* **9:**20-25.

Yoshitsugu H, Nishimura M, Tateno C, Kataoka M, Takahashi E, Soeno Y, Yoshizato K, Yokoi T, Naito S (2006) Evaluation of human CYP1A2 and CYP3A4 mRNA expression in hepatocytes from chimeric mice with humanized liver. *Drug Metab Pharmacokinet* **21:**465-474.

Zaiss A, Foley EM, Lawrence R, Schneider LS, Hoveida H, Secrest P, Catapang AB, Yamaguchi Y, Alemany R, Shayakhmetov DM, Esko JD, Herschman HR (2015) Hepatocyte heparan sulfate is required for adeno-associated virus 2 but dispensable for adenovirus 5 liver transduction in vivo. *J Virol* **pii: JVI.01939-15:**[Epub ahead of print].

Zangar R, Bollinger N, Verma S, Karin NJ, Lu Y (2008) The nuclear factor-kappa B pathway regulates cytochrome P450 3A4 protein stability. *Mol Pharmacol* **73:**1652-1658.

Zanger U, Schwab M (2013) Cytochrome P450 enzymes in drug metabolism: regulation of gene expression, enzyme activities, and impact of genetic variation. *Pharmacol Ther* **138:**103-141.

Zhang Y, Chirmule N, Gao GP, Qian R, Croyle M, Joshi B, Tazelaar J, Wilson JM (2001) Acute cytokine response to systemic adenoviral vectors in mice is mediated by dendritic cells and macrophages. *Mol Ther* **3:**697-707.

Zundler S, Neurath MF (2015) Interleukin-12: Functional activities and implications for disease. *Cytokine Growth Factor Rev* **26:**559-568.

**Footnotes**

This work was supported by research grants R21GM69870 from the National Institute of General Medical Sciences (M.A.C.), U01AI078045 from the National Institute of Allergy and Infectious Disease (M.A.C.) and the James W. McGinity Graduate Fellowship and the Williams & McGinity Graduate Fellowship (K. J.-S.).

**Legends for Figures**

**Figure 1. Live and Inactivated Recombinant Adenoviruses Activate Certain Signal Transduction Pathways in the Liver.** Gene profiling was performed on liver tissue isolated from male Sprague Dawley 4 days after a single dose ($5.7 \times 10^{12}$ viral particles per kilogram (vp/kg)) of virus. Representative gene expression arrays and densitometric profiles for each treatment group at this timepoint are illustrated here. Highlighted boxes represent genes associated with five different pathways that were significantly elevated in 3 of the 4 treatment groups with respect to saline treated controls. Housekeeping genes are located in the bottom horizontal row of each array and were utilized for normalization and analysis. The primary virus used in this study was a first generation adenovirus, expressing the *E. coli* beta-galactosidase transgene (AdlacZ). The early region 1 (E1, involved in virus replication) and early region 3 (E3, involved in evasion of the host immune response) in the genome were removed in this vector to accommodate the beta-galactosidase transgene cassette. A PEGylated version of this virus (PEGAd), which has a significantly lower immunological profile (Croyle, 2001; Croyle, 2002) and an inactive control, AdlacZ inactivated by exposure to riboflavin and UV light (UVAd) (Callahan, 2008b), were included to study the effect of the immune response against virus capsid proteins and virus receptor interactions on signal transduction patterns during infection. A helper-dependent adenoviral vector (HDAd), devoid of all viral genes containing the beta-galactosidase transgene (Croyle, 2005), was also included to fully study the effect of viral gene expression on signal transduction in the liver.

**Figure 2. Systemic Administration of a RGD-Deleted Recombinant Adenovirus Does Not Alter Hepatic CYP3A Expression and Function in Mice.** Catalytic activity, protein and

DMD Fast Forward. Published on February 11, 2016 as DOI: 10.1124/dmd.115.068874
This article has not been copyedited and formatted. The final version may differ from this version.



mRNA levels of hepatic CYP3A11 were evaluated 24 hours (Panels A, C and E respectively) and 48 hours (Panels B, D and F respectively) after systemic administration of $1 \times 10^{11}$ particles of either a first generation adenovirus expressing beta-galactosidase (AdlacZ) or a vector of the same generation expressing green fluorescent protein (GFP) with all arginine-glycine-aspartic acid (RGD) residues removed from capsid proteins (AdΔRGD). Data are reported as the means ± standard error of values obtained from 5 mice per treatment group at each timepoint. *$p < 0.05$ and **$p < 0.01$ with respect to vehicle control (phosphate-buffered saline, PBS).

**Figure 3. Hepatic Transduction Efficiency of a RGD-Deleted Recombinant Adenovirus in the Mouse.** Hepatic localization of transgene expression after a single dose of saline (first column), $1 \times 10^{11}$ particles of a first generation adenovirus expressing beta-galactosidase (AdlacZ, second column) or $1 \times 10^{11}$ particles of a vector of the same generation expressing green fluorescent protein (GFP) with RGD residues removed from capsid proteins (AdΔRGD, third column) or a GFP expressing first generation adenovirus (AdGFP, fourth column). (A) Liver section collected 24 hours after administration of phosphate-buffered saline. Endogenous beta-galactosidase expression could not be detected in sections from any animals in this treatment group (n=5). (B) Representative tissue section obtained 24 hours after administration of AdlacZ and stained with the histochemical substrate, X-gal. Cells containing the blue product generated by active beta-galactosidase in the presence of the substrate 5-bromo-4-chloro-3-indolyl-β-D-galactoside (X-gal) were considered positive for virus infection. Tissue section from mouse 24 hours after treatment with (C) AdΔRGD or AdGFP (D) and stained with X-gal. Beta-galactosidase expression was absent in sections from all animals within the two treatment group (n=5). (E) Hepatic tissue section from saline treated animal stained with an anti-GFP antibody.

Background staining for this transgene was not detected in sections obtained from all animals within this treatment group. (F) Tissue section from mice given a single dose of AdlacZ stained with an anti-GFP antibody. As noted for the saline controls, background staining for GFP was not detected in sections from this group. (G) Representative tissue section obtained 24 hours after administration of AdΔRGD and stained with anti-GFP antibody. Moderate levels of GFP were found in sections from each animal within this group as indicated by brown precipitate generated by the HRP conjugated antibody (n=5). (H) Liver tissue section from mice treated with AdGFP for 24 hours and stained for GFP using an anti-GFP antibody. (I) Liver section from mouse taken 48 hours after administration of a single dose of saline, stained with anti-GFP antibody. (J) Liver section taken 48 hours after a single dose of AdlacZ, stained with anti-GFP antibody. (K) Representative tissue section 48 hours after treatment with AdΔRGD stained with anti-GFP antibody. (L) Hepatic tissue section from mice treated with AdGFP for 48 hours and stained with an anti-GFP antibody. Magnification for all panels: 200 ×.

**Figure 4. Removal of RGD Epitopes from the Adenovirus Capsid Alters the Cytokine Secretion Profile and Elicits a Mild Increase in Serum Transaminases in the Mouse.** (A) Serum interleukin-6 levels measured 6, 24 and 48 hours after a single dose of saline (PBS) or $1 \times 10^{11}$ particles of either a first generation adenovirus expressing beta-galactosidase (AdlacZ) or a vector of the same generation expressing green fluorescent protein (GFP) with RGD residues removed from capsid proteins (AdΔRGD). (B) Forty-eight hour interleukin-12 secretion profile of mice given saline, AdlacZ or AdΔRGD. (C) Serum aspartate aminotransaminase (AST) profile 24 hours after administration of recombinant vectors. (D) Serum alanine aminotransaminase (ALT) profile 24 hours after a single dose of virus. (E) Serum AST levels 48

hours after administration of virus. (F) Serum ALT 48 hours after administration of virus. For each panel, data represent the means ± standard error of values obtained from 5 mice per treatment group at each timepoint. *$p < 0.05$, **$p < 0.01$ and ***$p < 0.001$ with respect to vehicle control (PBS).

**Figure 5. Virus-Mediated Changes in Gene and Protein Expression of Nuclear Receptors Regulating CYP3A4.** Gene expression of nuclear receptors PXR, RXRα, and CAR (Panels A, C, and E, respectively) and protein levels (Panels B, D, and F, respectively) in mice after 24 or 48 hours of infection with either AdlacZ or AdΔRGD. Mice were given saline (PBS) or $1 \times 10^{11}$ particles of either AdlacZ or AdΔRGD and gene and protein expression of nuclear receptors regulating CYP3A4 was assessed 24 and 48 hours post infection using qRT-PCR and Western Blot techniques, respectively. Data are reported as the means ± standard error of values obtained from 5 mice per treatment group at each timepoint. *$p < 0.05$ and **$p < 0.01$ with respect to vehicle control (PBS).

**Figure 6. Engagement of Integrin Receptors with a Non-Infectious Peptide Suppresses CYP3A4 Activity in HC-04 Cells.** (A) Catalytic activity of CYP3A after treatment with peptides containing either RGD or RGE sequences. Results are reported as the means ± standard error of values obtained from 3 culture plates per condition. *$p < 0.05$ with respect to saline-treated cells (control). (B) Histochemical staining for beta-galactosidase expression in hepatocytes infected with AdlacZ at a MOI of 100. Similar staining patterns were detected for cells treated with a control peptide containing an arginine-glycine-glutamic acid (RGE) sequence at a concentration of 1.5 mg/ml for 2 hours prior to infection. (C) Histochemical staining for

beta-galactosidase expression in hepatocytes treated with a RGD peptide (1.5 mg/ml). Peptide was added to culture media for 2 hours at 4°C prior to infection with AdlacZ at a MOI of 100. Original magnification of each panel: 200 ×.

**Figure 7. Silencing of β3 and/or β5 Integrin Subunits Reverses Adenovirus-Mediated Changes in CYP3A4.** (A) Degree of silencing achieved for each integrin subunit in HC-04 cells. Cells were transfected for 48 hours with either a non-targeting control siRNA (Control) or siRNA targeting either the αv, β3 or β5 subunit of the integrin receptor. Silencing was confirmed by qRT-PCR using primers specific for the different integrins. (B) CYP3A4 catalytic activity in HC-04 cells infected with adenovirus (MOI 500) for 72 hours after integrin silencing. Data depicted in Panel B was generated through comparison of CYP3A4 activity in virus-infected cells to activity in uninfected, saline-treated cells in which the same integrin subunit was silenced. Activity in the uninfected cells was normalized to 100% and data reported as activity which remained after virus infection (% remaining activity). Results are reported as the means ± standard error of values obtained from 3 culture plates per condition. **$p < 0.01$ with respect to siRNA control-treated cells, labeled as Control on the figure.

**Figure 8. Silencing of αv, β3 or β5 Integrin Subunits in the Absence of Virus Infection Decreases Gene Expression and Protein Levels of PXR and CAR but Not RXRα.** Gene expression levels of nuclear receptors: (A) PXR, (C) CAR, and (E) RXRα were assessed in HC-04 cells 48 hours after treatment with siRNA targeting either the αv, β3 or β5 subunit of the integrin receptor. Protein expression levels of (B) PXR, (D) CAR, and (F) RXRα in samples treated the same way as described above but harvested for protein and analyzed by Western Blot.

Values for control samples in these panels represent protein levels in HC-04 cells treated with non-targeting siRNA. Results are reported as the means ± standard error of values obtained from 3 culture plates per condition.

DMD Fast Forward. Published on February 11, 2016 as DOI: 10.1124/dmd.115.068874
This article has not been copyedited and formatted. The final version may differ from this version.



## Tables

**Table 1. Differential Expression Patterns of Genes Associated with Various Signal Transduction Pathways in the Liver Four Days After Administration of Recombinant Adenovirus.**[a] Numbers represent the ratio of the intensity of gene expression in a sample obtained from an animal given virus with respect to an animal given saline (vehicle control). Gene expression was normalized based on minimal background subtraction and interquartile normalization using ScanAlyze software and the GEArray Expression Analysis Suite. Bolded text corresponds with signal transduction pathways in arrays depicted in Figure 1.

| Gene | Pathway | AdlacZ | PEG | HDAd | UVAd |
|---|---|---|---|---|---|
| A2m | Jak-Stat | 0.754 | 3.232 | 0.710 | 1.705 |
| Bax | p53 | 0.697 | 1.634 | 2.745 | 2.361 |
| **Bcl2a1** | **NFκB** | **1.815** | **6.477** | **15.443** | **2.761** |
| Ccl2 | LDL | 0.865 | 1.971 | 0.944 | 1.074 |
| **Cend1** | **Wnt, PI3K** | **3.012** | **6.543** | **0.225** | **5.267** |
| Cdkn1a | p53 and Androgen | 0.685 | 1.573 | 0.044 | 2.682 |
| Cebpb | Insulin | 0.943 | 2.290 | 0.154 | 3.584 |
| Fos | Stress, CREB, PKC, PLC | 1.061 | 1.662 | 0.436 | 0.718 |
| **Ctsd** | **Retinoic acid, Estrogen** | **1.533** | **4.141** | **0.096** | **2.956** |
| Egfr | Estrogen, Androgen | 0.940 | 0.939 | 0.144 | 2.617 |
| Egfr1 | Mitogenic, CREB | 3.146 | 6.875 | 0.289 | 0.937 |
| Ei24 | p53 | 0.647 | 2.132 | 1.023 | 1.634 |
| Fasn | Insulin | 0.641 | 1.169 | 0.170 | 1.606 |
| Fn1 | PI3 Kinase/AKT | 0.628 | 1.480 | 0.029 | 1.954 |
| Gadd45a | p53 | 1.119 | 0.865 | 0.238 | 1.045 |
| Gys2 | Insulin | 0.746 | 1.614 | 0.059 | 1.563 |
| Hnf3b | Hedgehog | 1.223 | 1.532 | 0.400 | 1.363 |
| Hspb1 | Stress | 1.482 | 2.556 | 0.227 | 2.398 |
| Hspca | Stress | 1.575 | 3.839 | 0.144 | 3.279 |
| Icam1 | NFκB and Phospholipase C | 1.134 | 5.012 | 0.614 | 1.137 |
| Igfbp3 | p53 | 0.382 | 0.877 | 1.708 | 2.834 |
| Il4r | Jak-Stat | 1.085 | 1.674 | 0.211 | 1.814 |
| **Irf1** | **Jak-Stat** | **2.368** | **4.078** | **3.186** | **2.265** |
| **Jun** | **Wnt, PI3K/AKT, PKC** | **3.362** | **5.572** | **0.360** | **2.663** |
| Klk3 | Androgen | 0.417 | 1.481 | 0.633 | 1.177 |
| Tnfrsf6 | p53, NFAT | 1.646 | 0.756 | 0.794 | 0.781 |
| Lta | NFκB | 1.297 | 0.396 | 0.497 | 0.837 |
| Mdm2 | p53 | 4.117 | 4.066 | 3.854 | 2.040 |

| | | | | | |
|---|---|---|---|---|---|
| **Mig** | **Jak-Stat** | **3.984** | **3.395** | **7.851** | **1.862** |
| Myc | Wnt, Stress, PKC | 0.922 | 1.774 | 0.923 | 1.773 |
| **Nfkb1** | **NFκB** | **1.782** | **3.501** | **3.788** | **1.429** |
| Nfkbia | NFκB | 2.209 | 1.775 | 0.592 | 1.479 |
| Nos2 | Jak-Stat, NFκB, PLC | 2.699 | 0.510 | 2.267 | 1.517 |
| **Odc1** | **PKC** | **3.527** | **2.822** | **4.258** | **1.311** |
| **Pten** | **PI3 Kinase/AKT** | **3.605** | **1.400** | **8.479** | **1.975** |
| **Rbp1** | **Retinoic acid** | **1.443** | **2.236** | **1.935** | **2.271** |
| Vcam | NFκB, PKC, LDL | 1.804 | 0.879 | 1.461 | 0.258 |

[a]Descriptions of vectors can be found in the Figure 1 legend

# Figure 1

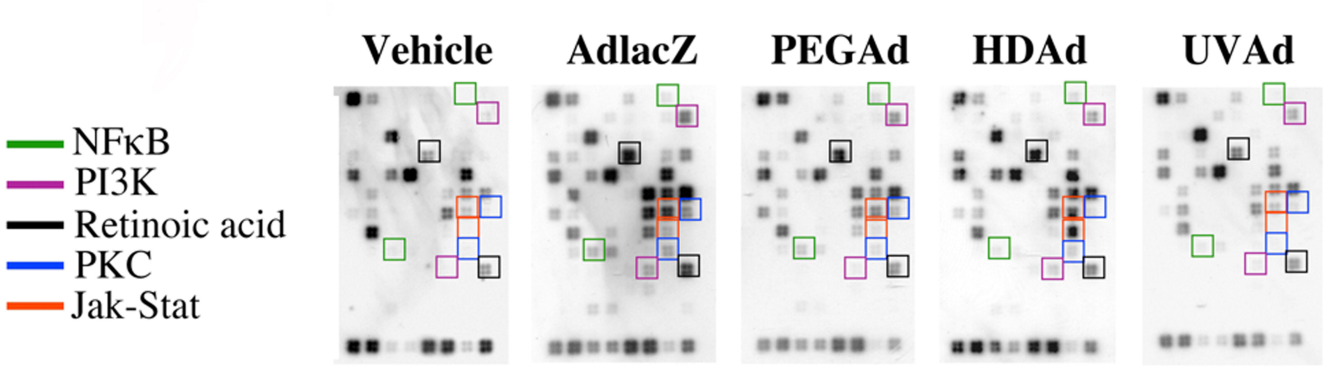
Vehicle
AdlacZ
PEGAd
HDAd
UVAd
NFκB
PI3K
Retinoic acid
PKC
Jak-Stat

# Figure 2

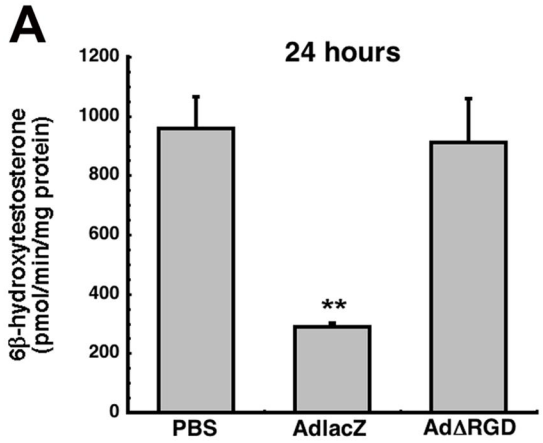
A
24 hours
6β-hydroxytestosterone (pmol/min/mg protein)
1200
1000
800
600
400
200
0
**
PBS
AdlacZ
AdΔRGD

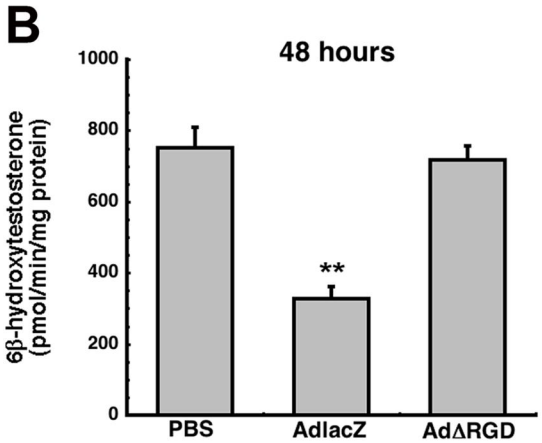
B
48 hours
6β-hydroxytestosterone (pmol/min/mg protein)
1000
800
600
400
200
0
**
PBS
AdlacZ
AdΔRGD

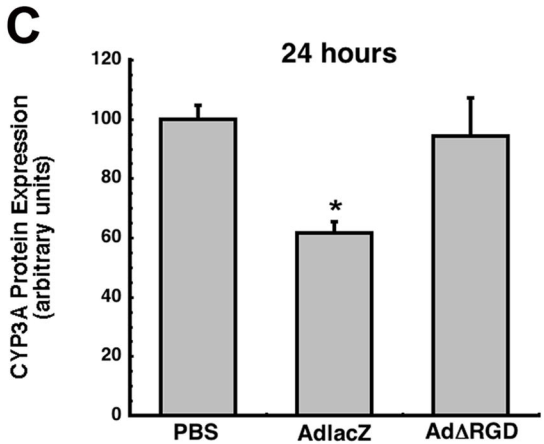
C
24 hours
CYP3A Protein Expression (arbitrary units)
120
100
80
60
40
20
0
*
PBS
AdlacZ
AdΔRGD

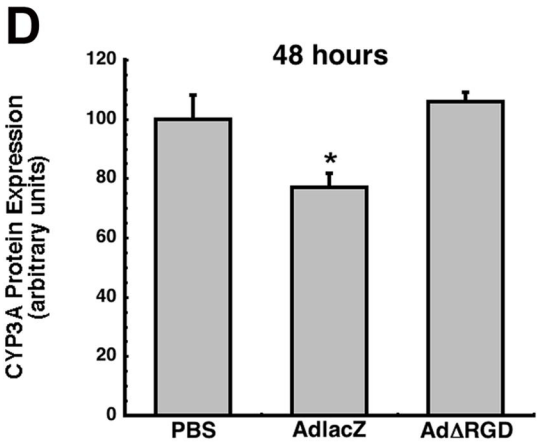
D
48 hours
CYP3A Protein Expression (arbitrary units)
120
100
80
60
40
20
0
*
PBS
AdlacZ
AdΔRGD

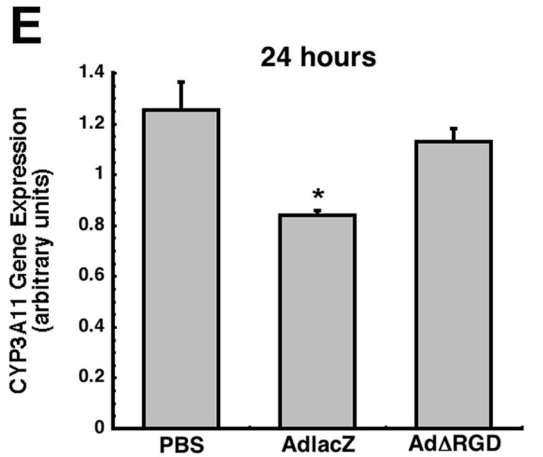
E
24 hours
CYP3A11 Gene Expression (arbitrary units)
1.4
1.2
1
0.8
0.6
0.4
0.2
0
*
PBS
AdlacZ
AdΔRGD

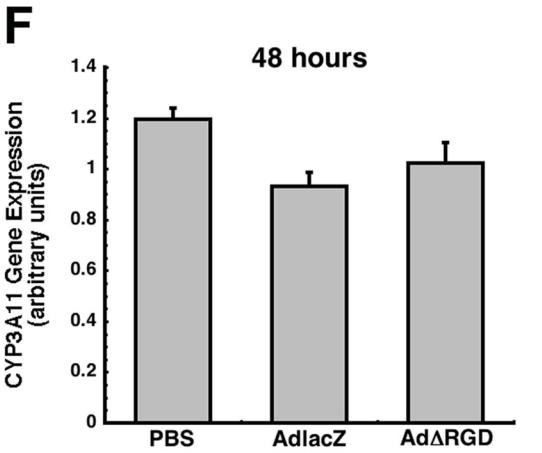
F
48 hours
CYP3A11 Gene Expression (arbitrary units)
1.4
1.2
1
0.8
0.6
0.4
0.2
0
PBS
AdlacZ
AdΔRGD

# Figure 3

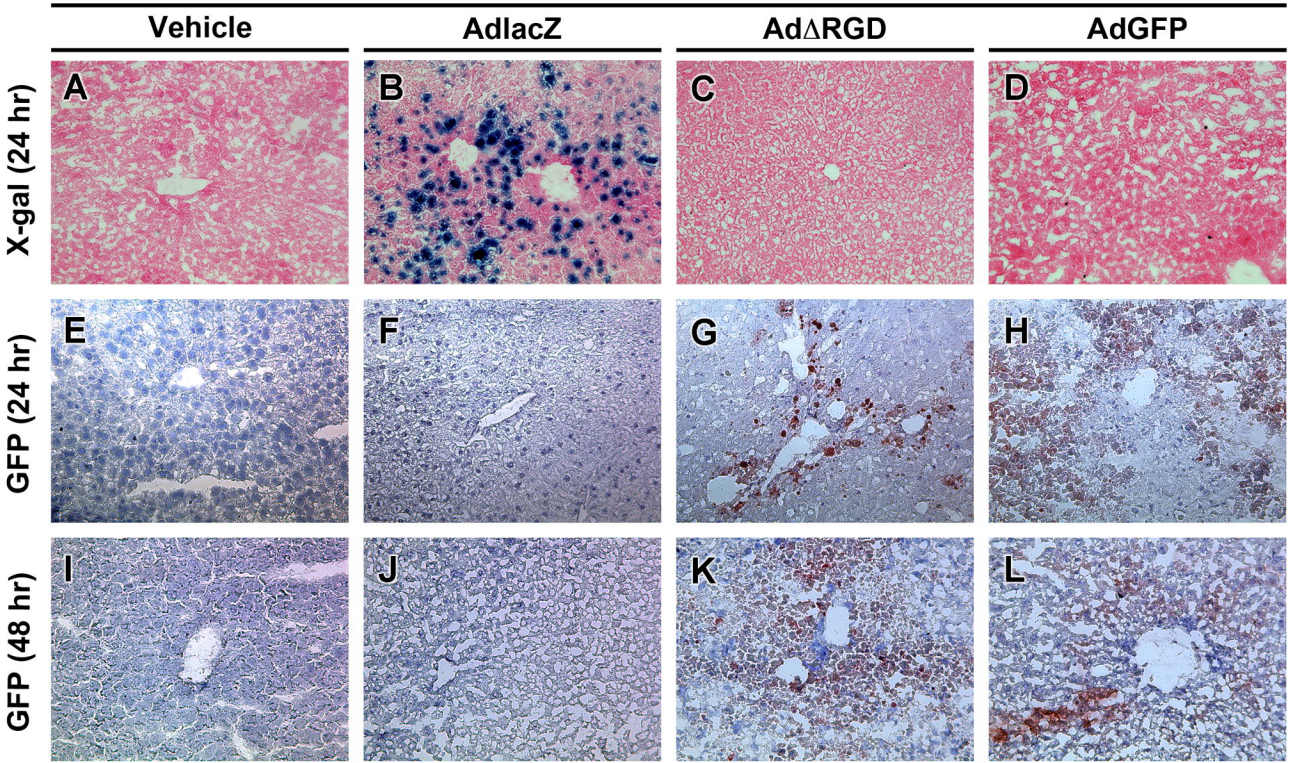
Vehicle
AdlacZ
AdΔRGD
AdGFP
X-gal (24 hr)
GFP (24 hr)
GFP (48 hr)
A
B
C
D
E
F
G
H
I
J
K
L

# Figure 4

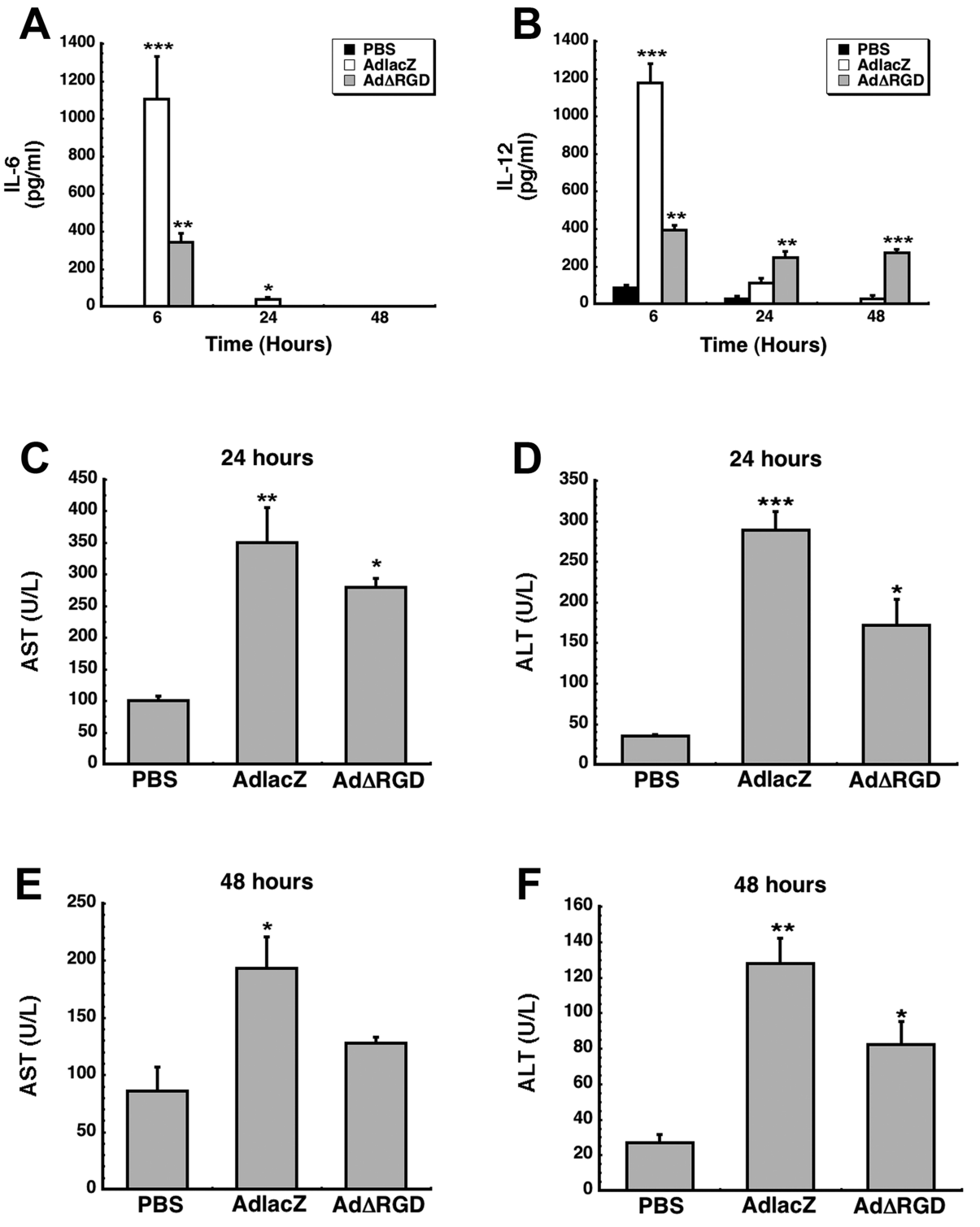
A
IL-6 (pg/ml)
1400
1200
1000
800
600
400
200
0
***
**
*
PBS
AdlacZ
AdΔRGD
6
24
48
Time (Hours)
B
IL-12 (pg/ml)
1400
1200
1000
800
600
400
200
0
***
**
**
***
PBS
AdlacZ
AdΔRGD
6
24
48
Time (Hours)
C
24 hours
AST (U/L)
450
400
350
300
250
200
150
100
50
0
**
*
PBS
AdlacZ
AdΔRGD
D
24 hours
ALT (U/L)
350
300
250
200
150
100
50
0
***
*
PBS
AdlacZ
AdΔRGD
E
48 hours
AST (U/L)
250
200
150
100
50
0
*
PBS
AdlacZ
AdΔRGD
F
48 hours
ALT (U/L)
160
140
120
100
80
60
40
20
0
**
*
PBS
AdlacZ
AdΔRGD

# Figure 5

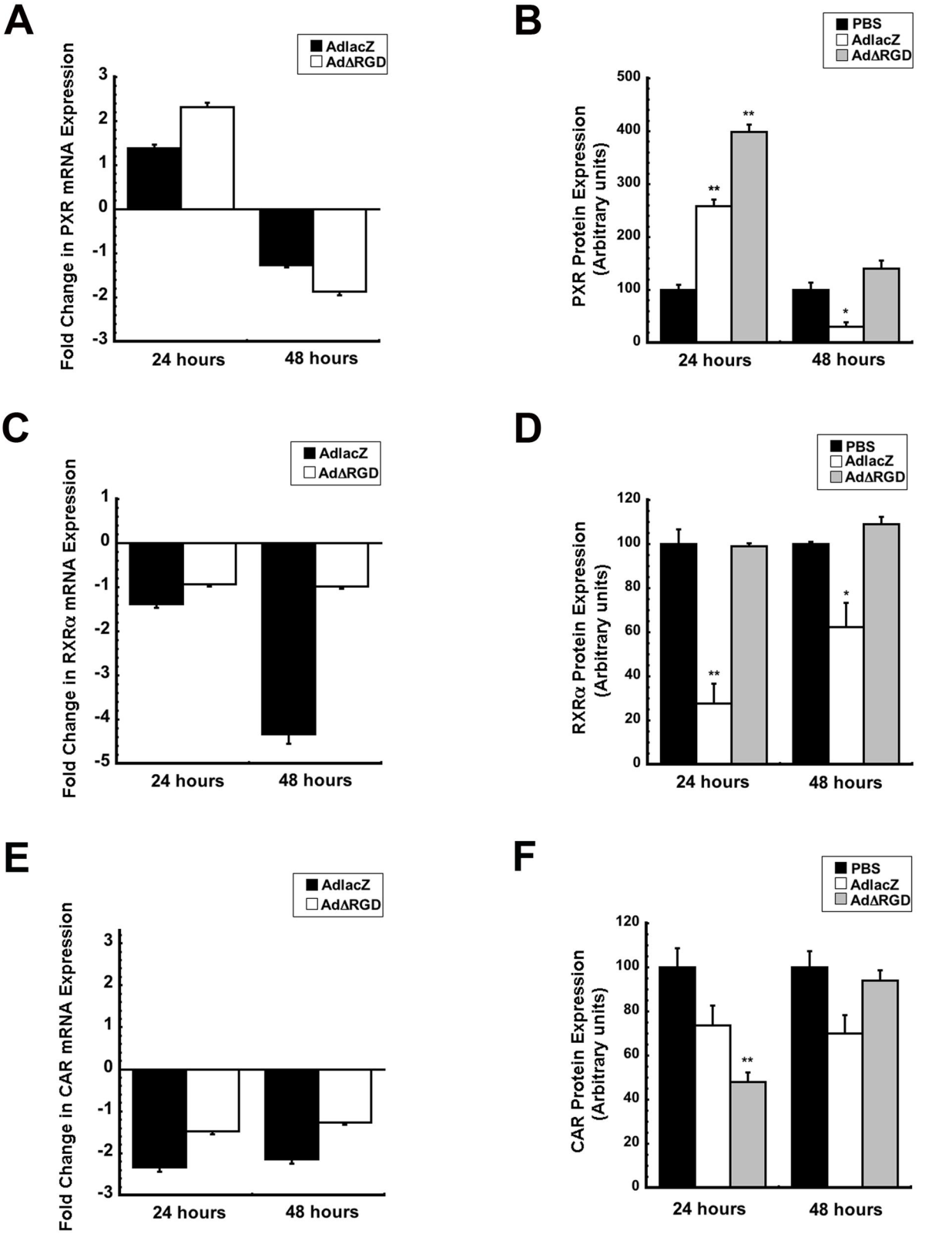
A
AdlacZ
AdΔRGD
Fold Change in PXR mRNA Expression
3
2
1
0
-1
-2
-3
24 hours
48 hours
B
PBS
AdlacZ
AdΔRGD
PXR Protein Expression (Arbitrary units)
500
400
300
200
100
0
**
**
*
24 hours
48 hours
C
AdlacZ
AdΔRGD
Fold Change in RXRα mRNA Expression
1
0
-1
-2
-3
-4
-5
24 hours
48 hours
D
PBS
AdlacZ
AdΔRGD
RXRα Protein Expression (Arbitrary units)
120
100
80
60
40
20
0
**
*
24 hours
48 hours
E
AdlacZ
AdΔRGD
Fold Change in CAR mRNA Expression
3
2
1
0
-1
-2
-3
24 hours
48 hours
F
PBS
AdlacZ
AdΔRGD
CAR Protein Expression (Arbitrary units)
120
100
80
60
40
20
0
**
24 hours
48 hours

Figure 6

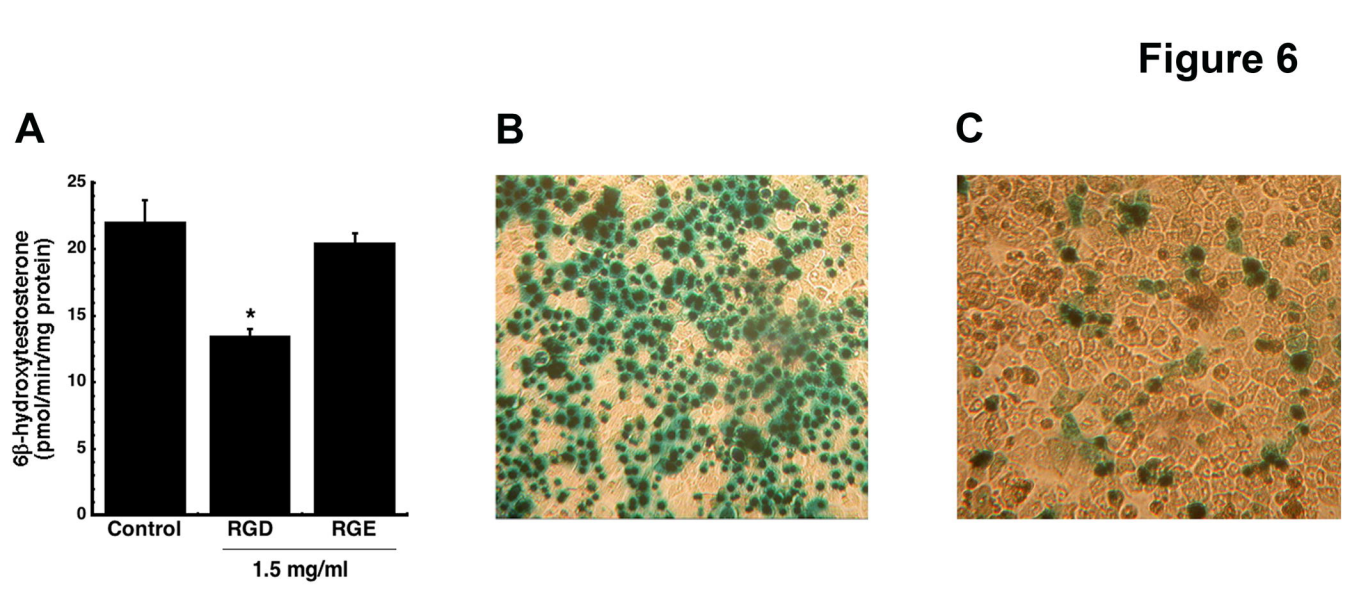
A
B
C
6β-hydroxytestosterone (pmol/min/mg protein)
25
20
15
10
5
0
*
Control
RGD
RGE
1.5 mg/ml

Figure 7


A
Fold Reduction mRNA Expression
0
1
2
3
4
5
αv siRNA
β3 siRNA
β5 siRNA
αvβ3 siRNA (αv)
αvβ3 siRNA (β3)
αvβ5 siRNA (αv)
αvβ5 siRNA (β5)
B
Remaining CYP3A4 Activity (%)
0
20
40
60
80
100
**
**
**
**
Control
αv siRNA
β3 siRNA
β5 siRNA
αvβ3 siRNA
αvβ5 siRNA

# Figure 8

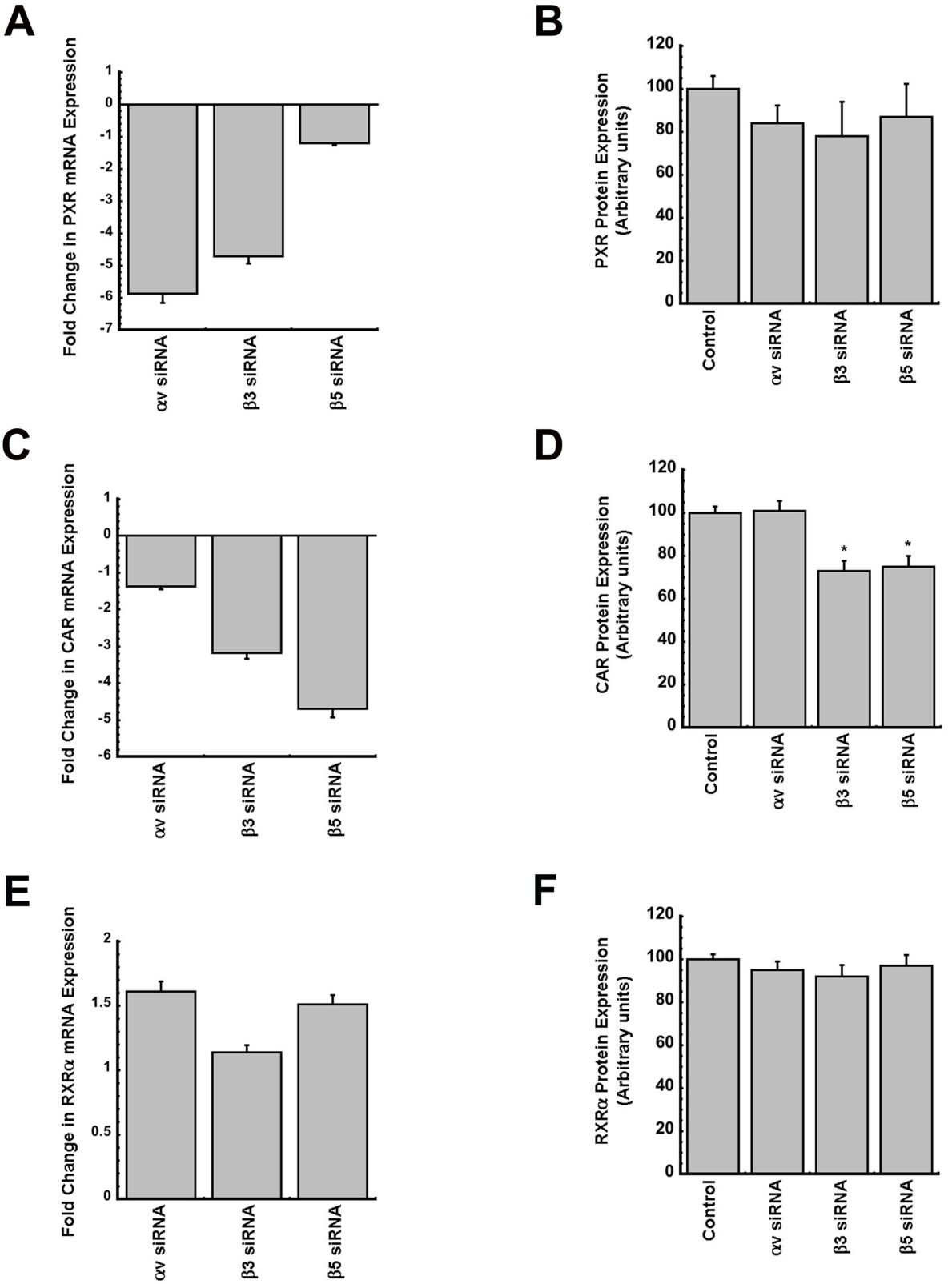
A
Fold Change in PXR mRNA Expression
1
0
-1
-2
-3
-4
-5
-6
-7
αv siRNA
β3 siRNA
β5 siRNA
B
PXR Protein Expression (Arbitrary units)
120
100
80
60
40
20
0
Control
αv siRNA
β3 siRNA
β5 siRNA
C
Fold Change in CAR mRNA Expression
1
0
-1
-2
-3
-4
-5
-6
αv siRNA
β3 siRNA
β5 siRNA
D
CAR Protein Expression (Arbitrary units)
120
100
80
60
40
20
0
*
*
Control
αv siRNA
β3 siRNA
β5 siRNA
E
Fold Change in RXRα mRNA Expression
2
1.5
1
0.5
0
αv siRNA
β3 siRNA
β5 siRNA
F
RXRα Protein Expression (Arbitrary units)
120
100
80
60
40
20
0
Control
αv siRNA
β3 siRNA
β5 siRNA